NAVY DEPARTMENT

THE DAVID W. TAYLOR MODEL BASIN

WASHINGTON 7, D.C.

THE MEASUREMENT OF OSCILLATING PRESSURES

IN THE VICINITY OF PROPELLERS

by

A. J. Tachmindji and M. C. Dickerson

[redacted]

[redacted]

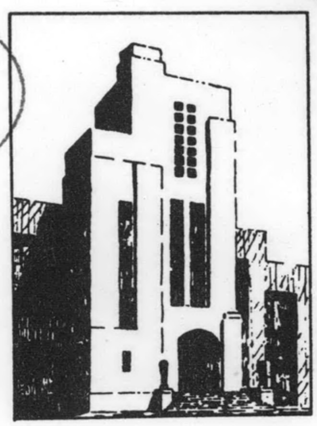

RESEARCH AND DEVELOPMENT REPORT

APRIL 1957

Report No. 1130

THE MEASUREMENT OF OSCILLATING PRESSURES IN THE VICINITY OF PROPELLERS

by

A. J. Tachmindji and M. C. Dickerson

Research and Development Report

April 1957 Report No. 1130

TABLE OF CONTENTS

LIST OF FIGURES

TABLE OF SYMBOLS

$b_{0.7}$ = Section length at 0.7 radius

d = Propeller diameter

e = Propeller efficiency

J = $\frac{V}{nd}$ = Speed coefficient

K_t = $\frac{T}{\rho n^2 d^4}$ = Thrust coefficient

K_p = $\frac{p}{\rho n^2 d^2}$ = Pressure coefficient at blade frequency

K_{p_t} = $\frac{p_t}{\rho n^2 d^2}$ = Total pressure coefficient

K_q = $\frac{Q}{\rho n^2 d^5}$ = Torque coefficient

m = Index of summation

n = Revolutions per unit time

p = Oscillating pressure at blade frequency for a point in space (single amplitude)

p_t = Total oscillating pressure at blade frequency and higher harmonics for a point in space (single amplitude)

Q = Propeller torque

R_e = $\frac{b_{0.7}\left[V^2 + (0.7\pi nd)^2\right]^{1/2}}{\nu}$ = Reynolds number

T = Propeller thrust

t = $z - \frac{d}{2}$ = Vertical clearance from propeller tip

V = Water velocity

x = Axial co-ordinate from propeller plane (positive direction is forward of propeller, Figure 5)

y = Horizontal co-ordinate (positive to starboard for R.H. Propeller, Figure 5)

z = Vertical co-ordinate (positive upwards, Figure 5)

Z = Number of blades

α_β = Blade angle for maximum pressure (measured from z-axis in the direction of propeller rotation)

λ = Index of summation

ν = Kinematic viscosity

ρ = Density

ABSTRACT

This report gives the results of the oscillating pressures measured at points in the free-stream, both ahead and behind the propellers and on an imaginary plane parallel to the propeller axis. The effect of rpm, propeller loading and speed coefficient have been investigated. Results have been obtained for the effect of blades both at blade frequency and higher harmonics. The oscillating pressure for a four-bladed propeller has been calculated using the pressure signal of a single blade and compared to the experimental values.

INTRODUCTION

Hydrodynamic pressure fluctuations in the vicinity of a propeller have become a very important problem with the increasing use of high powers, and result in associated effects of vibration* and noise. The oscillating pressures of a rotating propeller are occurring predominantly at blade frequency (revolutions per minute times the number of blades), but higher harmonics can also be detected. Although the magnitude of these pressures is small, the area in the vicinity of the stern on which they can act can be large, thus resulting in sizable vibratory forces on the hull structure. These forces are transmitted to the hull surface through the water and are known as "surface forces"[1].

The presence of the oscillating pressure fields in the vicinity of propellers is also important in determining the effect of propeller design parameters on the noise signal emitted by the propeller.

Up to the present time, however, little experimental information has been published which would enable the designer to predict these pressures in the critical region of the propeller tips, to determine the stern arrangements and the effects of clearances between the propeller and the surrounding structure. F. M. Lewis[2] used the electrical analogy technique to map pressure field contours in the vicinity of a three-bladed propeller. Theoretical work conducted by Breslin[3] afforded a means of estimating the oscillating pressures produced by the thrust contribution of the propeller, in the absence of external surfaces.

Theoretical work has also been conducted in the field of aircraft propellers by Gutin[4] who derived equations which were useful only at a large distance from the propeller. Gutin's fundamental equations have, however, been used by Hubbard and Regier[5], Garrick[6] and Watkins[7] who obtained solutions which make possible the prediction of oscillating pressures at any point in space. Additional theoretical work was also conducted by Deming[8], Lieber[9], and others.

* This work is of direct interest to the Hydro - Elasticity Panel of SNAME

1 References are listed on Page 8

Experimental information on this subject has, however, been lacking and it is for this reason that it was decided to undertake the measurement of the free space oscillating pressures in the vicinity of marine propellers. The purpose of the tests was to determine the amplitude and phase of these pressures, their laws of similitude and the magnitude of the harmonics higher than blade frequency. Tests were also conducted to determine the effect of tip clearances, axial clearances and number of blades.

This report gives the results of these tests for oscillating pressures measured on points in the free stream, both ahead and behind the propeller and on an imaginary plane parallel to the propeller axis. The effect of propeller loading and speed coefficient have also been investigated. All the results have been obtained for a propeller operating in a uniform velocity field. Results for a propeller operating in a variable inflow field have been previously reported[10].

INSTRUMENTATION AND PROCEDURE

The tests were conducted in the 12-inch Variable Pressure Water Tunnel at DTMB and the pressure measurements obtained by means of a Hathaway pressure gauge having a maximum range of $\pm$ 0.5 psi. Additional tests were also conducted with a propeller operating in the basin in open water in order to determine any tunnel interference effects. Measurements were conducted with four propellers having the characteristics given in Table I.

TABLE I

Propeller No.	3192	2714	3192	3192
No. of blades	4	3	2	1
Diameter (in)	7.26	8.17	7.26	7.26
p/d (0.7R)	1.00	1.06	1.00	1.00
MWR	0.323	0.464	0.323	0.323
Exp. Area Ratio	0.607	0.718	0.303	0.151
Hub Dia Ratio	0.263	0.191	0.263	0.263
Rotation	RH	RH	RH	RH

The geometric and performance characteristics of Propeller 2714 are given in Figures 1 and 2 and for Propeller 3192 in Figures 3 and 4. However, it should be noted that the pitch distribution shown in Figure 3 is that corresponding to a pitch ratio of 0.744 at 0.7R.

The pressure gauge was located in the free stream, external to the propeller slipstream, its position relative to the propeller center being given by the co-ordinates x, y and z according to the co-ordinate system shown in Figure 5. The details of the instrumentation used during the tests for determining the amplitude and phase of the blade frequency component and the magnitude of the higher harmonics have already been described in Reference 10.

Tests were conducted with these propellers having a pressure at the axis of 35.3 ft. of water absolute and operating at different speed coefficients (J) for a range of revolutions per minute. Measurements of the rpm, water speed, and thrust were obtained for each condition. The oscillating pressure signal was recorded on a Consolidated oscillograph, while the amplitude and phase of the blade frequency component was obtained from the vibration analyzer. Measurements of the harmonic components of frequencies different than blade frequency was accomplished by using a General Radio Wave Analyzer and by performing harmonic analyses of the recorded oscillograph records. No attempts have been made to measure the mean pressures at points in space.

RESULTS

The test results are presented in a non-dimensional form as

$$K_p = \frac{p}{\rho n^2 d^2} \qquad (1)$$

and

$$K_{p_t} = \frac{p_t}{\rho n^2 d^2} \qquad (2)$$

where
- p = pressure oscillation (single amplitude) at blade frequency
- p_t = total pressure oscillation (single amplitude) (all frequencies)
- n = revolutions per second
- d = propeller diameter
- ρ = density

The phase relationship (α_β) between the oscillating pressure and the propeller blade is defined as the blade angle for maximum pressure and is measured from the z-axis in the direction of propeller rotation.

Effect of RPM

Tests were conducted on Propeller 2714 at different speed coefficients (J) and over a range of rpm from 800 to 1200. The conditions were duplicated with the propeller operating in open water in the basin and over the same rpm range.

Figure 6 shows the variation in K_p and α_β with rpm for different speed coefficients and for a single point in space. It is seen that results are dependent only on the non-dimensional coefficient J and are independent of speed for a sufficiently high Reynolds number.

The test results obtained with the propeller operating in open water agreed well within experimental limits with those obtained in the tunnel, provided thrust and torque measurements were the same.

On the basis of this information it was decided to conduct all further measurements in the 12-inch tunnel at a constant value of 900 rpm.

Effect of Clearances

The free space oscillating pressures at blade frequency were obtained with Propeller 2714 for four values of speed coefficient and for a range of space co-ordinates x, y and z. Figures 7 and 8 show the variation in amplitude and phase of the oscillating pressure signal along an imaginary line parallel to the propeller axis and having the co-ordinates y/d = 0 and t/d = 0.098. In these figures, the horizontal scale x/d denotes distances from the plane of rotation; positive values denote distances ahead of the propeller plane and negative values denote positions behind it. Figures 9 and 10 show the variation of this pressure along an imaginary line in the propeller plane at a distance of 0.098 d from the tips. Figures 11, 12, 13, and 14 indicate the variation of oscillating pressure with varying tip clearance for planes ahead and behind the propeller plane.

It is noted that maximum pressure amplitude occurs not at the plane of rotation but somewhat ahead of it, at a distance of about 15% of the diameter. This is to be expected, as the largest percentage of the thrust is developed by suction. The position of this maximum, however, will be dependent on the speed coefficient of the propeller, the radial distribution of circulation and the shape of the propeller tips.

Effect of Number of Blades

In order to investigate the effect of number of blades and to be able to separate this effect from other variables such as pitch distribution, blade form, etc. it was decided to use a propeller with removable blades. Propeller 3192 was, therefore, tested with one, two and four blades in order to determine its characteristics and the effect of number of blades on the oscillating pressure. Figure 15 shows typical oscillograph records for each number of blades and for two values of speed coefficient. It is noted that the signal from the one-bladed propeller consists of a relatively large number of harmonics. As, however, the number of blades is increased the harmonics higher than blade frequency decrease in amplitude and the total pressure signal is primarily composed of one frequency. This effect is shown in Figure 16, where the ratio of the blade frequency pressure amplitude (p) to the amplitude of the total pressure signal (p_t) is plotted as a function of number of blades. For a large number of blades, therefore, the total pressure amplitude can be considered as being equal to the amplitude at blade frequency.

The variation of the blade frequency component for the one, two and four bladed propeller is shown in Figure 17 for various values of speed coefficient. Although it is seen that K_p generally increases with increasing number of blades, it should be noted that the three propellers do not deliver the same thrust at the same J. The ratio K_p / K_t is, therefore, plotted in Figure 18 indicating that the pressure oscillation at blade frequency decreases slightly with increasing Z. On the same figure is plotted K_{p_t}/K_t and shows a rapid decrease of the total pressure with increasing number of blades.

For propellers having more than four blades, the curves of K_p/K_t will tend to follow asymptotically K_{p_t} / K_t and this decrease with increasing Z is therefore, expected to become more rapid.

Higher Harmonics

Up to the present we have been primarily concerned with the amplitude of the pressure oscillations at blade frequency and with the amplitude of the total pressure oscillations. It is, however, of interest to examine the harmonic content of the total pressure signal and for this reason harmonic analyses of the oscillograph records were performed. Typical results are shown in Figures 19, 20 and 21 for the propellers having one, two and four blades and for J = 0.3, 0.6, 0.7 and 0.8. The higher harmonics are expressed as a percentage of the blade frequency components and it is noted that for the one-bladed propeller the 10th harmonic is about 10% of the amplitude at blade frequency. The two and four bladed propellers, however, indicate a much lower percentage of the higher harmonics.

CORRELATION BETWEEN NUMBER OF BLADES

In most theoretical work it is usually assumed that the oscillating pressure at a point in the vicinity of a propeller having a finite number of blades, can be obtained by the pressure signal of a single blade and adding the effects of each other blade. It is, therefore, interesting to check this assumption and attempt to derive the pressure signal for a propeller having a large number of blades using the results obtained from a propeller with a single blade.

The total pressure oscillation for a single blade can be written as

$$p_t \;(1) = \sum_{m=1}^{\infty} p_m \cos(m \omega t + \epsilon_m) \qquad (3)$$

where p_m is the amplitude of the harmonic components and ϵ_m their phase relationships. For Z number of blades, p_t will become

$$p_t \;(Z) = \sum_{m=1}^{\infty} p_m \sum_{\lambda=1}^{Z} \cos\left[m\left(\omega t + \lambda \frac{2\pi}{Z}\right) + \epsilon_m\right]$$

$$= \sum_{m=1}^{\infty} Z \, p_{mz} \cos(m z \omega t + \epsilon_{mz}) \qquad (4)$$

Using such an analysis it is possible to derive the pressure signal of a four-bladed propeller using the results of the single and two-bladed propellers. It should be remembered, however, that the total thrust will increase with increasing number of blades but will not be proportional to Z.

The results of this computation are shown in Figure 22 in which the values of K_p/K_t for the blade frequency and for the second harmonic as obtained from the one and two-bladed propeller by means of the above analysis, are compared to the experimental results. It is noted that the agreement between the experimental and computed values is reasonably good.

Using a similar approach, the blade frequency free-space oscillating pressure has been estimated for a propeller having various number of blades (up to Z = 10). The results which are shown in Figure 23, have been obtained from the one, two and four-bladed propellers. The values cannot, of course, be considered completely accurate and can only be used to indicate the order of magnitude. Furthermore, it should be emphasized, that they were derived from a propeller having a specific blade outline and pitch distribution and cannot necessarily be used for all propellers.

CONCLUSION

This report gives the results of the free-space oscillating pressures in the vicinity of a propeller. It should be emphasized, that the amplitude of the oscillating pressures on a rigid surface at the same points will be substantially larger than the free-space pressures. The increase will depend on the shape, configuration and position of the surface, and can be obtained by considering an image propeller on the other side of the surface such that the boundary conditions on the surface are satisfied. For example, the oscillating pressures on a fixed plane parallel to the x-axis will be twice the free-space oscillating pressure. In this case, the image propeller will be similar and equidistant from the plane to the propeller under consideration. In general, however, the image will be distorted in such a way as to satisfy the boundary conditions on the surface.

The results show that the oscillating pressures can be measured with good accuracy (down to 0.005 psi) for frequencies less than 300 cps. Furthermore, the similarity laws are satisfied provided the Reynolds number is sufficiently high.

The results obtained to show the effect of clearances indicate that the maximum free-space oscillating pressure occurs some 15% of the diameter ahead of the plane of rotation when the propeller is operating at its design speed coefficient.

The effect of number of blades indicates that the percentage of the blade frequency component to the total oscillating pressure for all frequencies, increases with increasing number of blades. The amplitude of both, however, decreases with higher number of blades.

It has also been shown that it is possible to predict approximately the magnitude of the free-space oscillating pressure for a propeller having a large number of blades when the results of a similar propeller with less blades are known.

The results given in this report are applicable only to the free-space oscillating pressures for the tested propellers and are not necessarily applicable to other propellers or to similar propellers operating in a wake distribution.

REFERENCES

1. Lewis, F. M. and Tachmindji, A. J. "Propeller Forces Exciting Hull Vibrations" Trans. SNAME, 1954

2. Lewis, F. M., "Propeller Vibration" Trans. SNAME, 1935

3. Breslin, J. P., "The Unsteady Pressure Field near a Ship Propeller and the Nature of the Vibratory Forces Produced on an Adjacent Surface" Stevens Institute of Technology, ETT Report No. 609, 1956

4. Gutin, L., "On the Sound Field of a Rotating Propeller" NACA TM 1195, 1948 or Phys. Zeitschr der Sowjetunion Bd 9, Heft 1, 1936, pp 57-71

5. Hubbard, H. H. and Regier, A. A. "Free-Space Oscillating Pressures Near the Tips of Rotating Propeller" NACA Report 996, 1950

6. Garrick, I. E. and Watkins, C. E., "A Theoretical Study of the Effect of the Forward Speed on the Free-Space Sound Pressure Field Around Propellers" NACA TN 3018

7. Watkins, C. E. and Durling, B.J., "A Method for Calculation of Free-Space Sound Pressures near a Propeller in Flight Including Considerations of the Chordwise Blade Loading" NACA TN 3809, 1956

8. Deming, A. F. "Propeller Rotation Noise Due to Torque and Thrust" NACA TN 747, 1940

9. Lieber, P., Grubin, C. and Wan, K. S., "A Theoretical Investigation of Aerodynamic Forces Generated by a Propeller on an Airfoil Situated Upstream" WADC Tech Report 53-494, 1953, (Part I and II)

10. Tachmindji, A. J. and Dickerson, M. C., "The Measurement of Thrust Fluctuation and Free-Space Oscillating Pressures for a Propeller" DTMB Report 1107, 1957

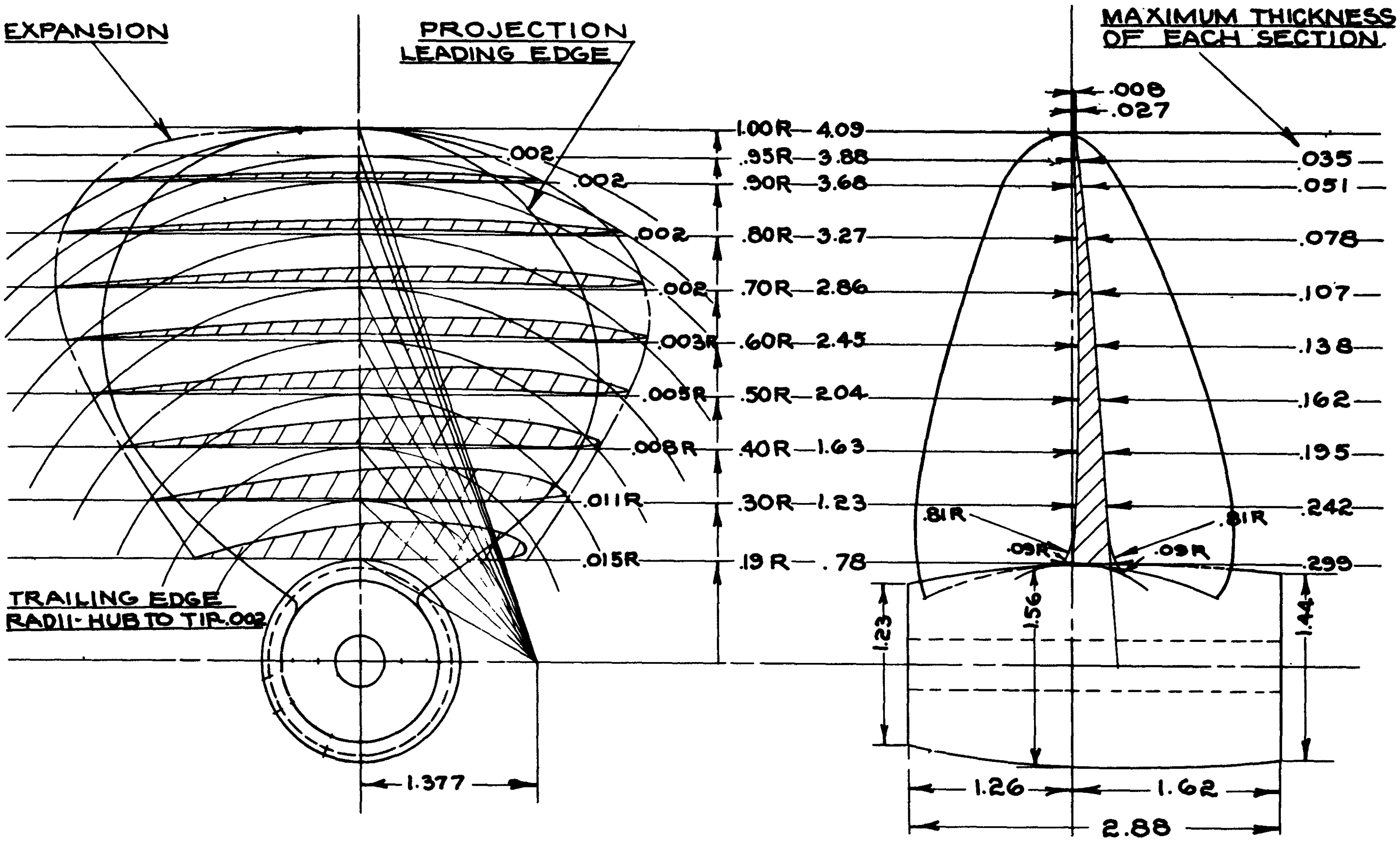

NUMBER OF BLADES	3
EXP. AREA RATIO	0.718
MWR	0.464
BTF	VAR.

HUB DIAMETER RATIO ..	0.191
PITCH RATIO	1.059
DIAMETER	8.170ins
PITCH	8.650ins.
ROTATION	R.H

Figure 1 - Geometric Characteristics of Propeller 2714

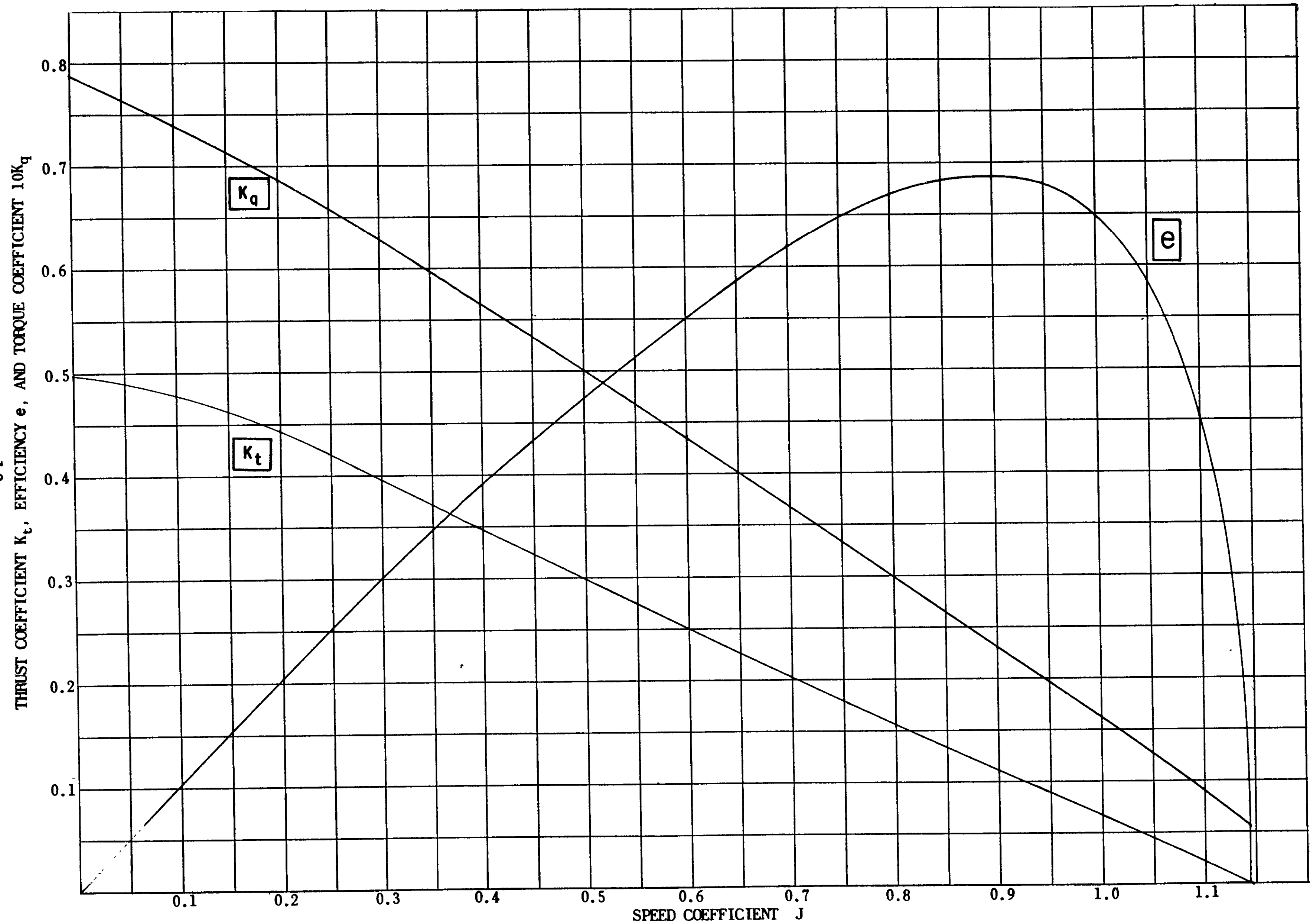

Figure 2 - Performance Characteristics of Propeller 2714

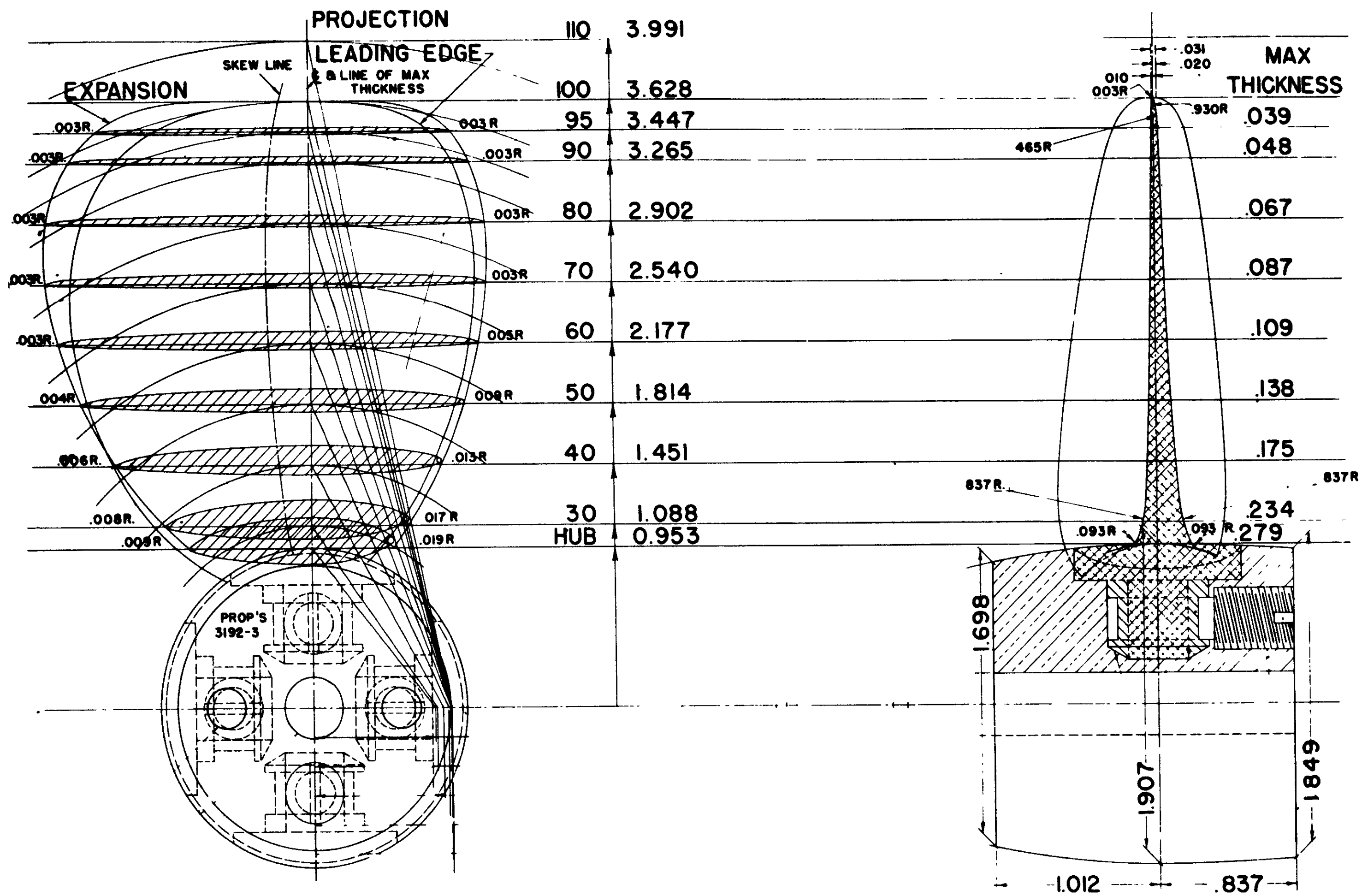

EXPANDED AREA RATIO

1 BLADE	0.151
2 BLADE	0.303
4 BLADE	0.607

RIGHT HAND ROTATION

MWR	0.323
BTF	VAR.
TEST PITCH RATIO	1.000 @ 0.7R
DESIGN PITCH RATIO	0.744 @ 0.7R
DIAMETER	7.256 ins.

Figure 3 - Geometric Characteristics of Propeller 3192

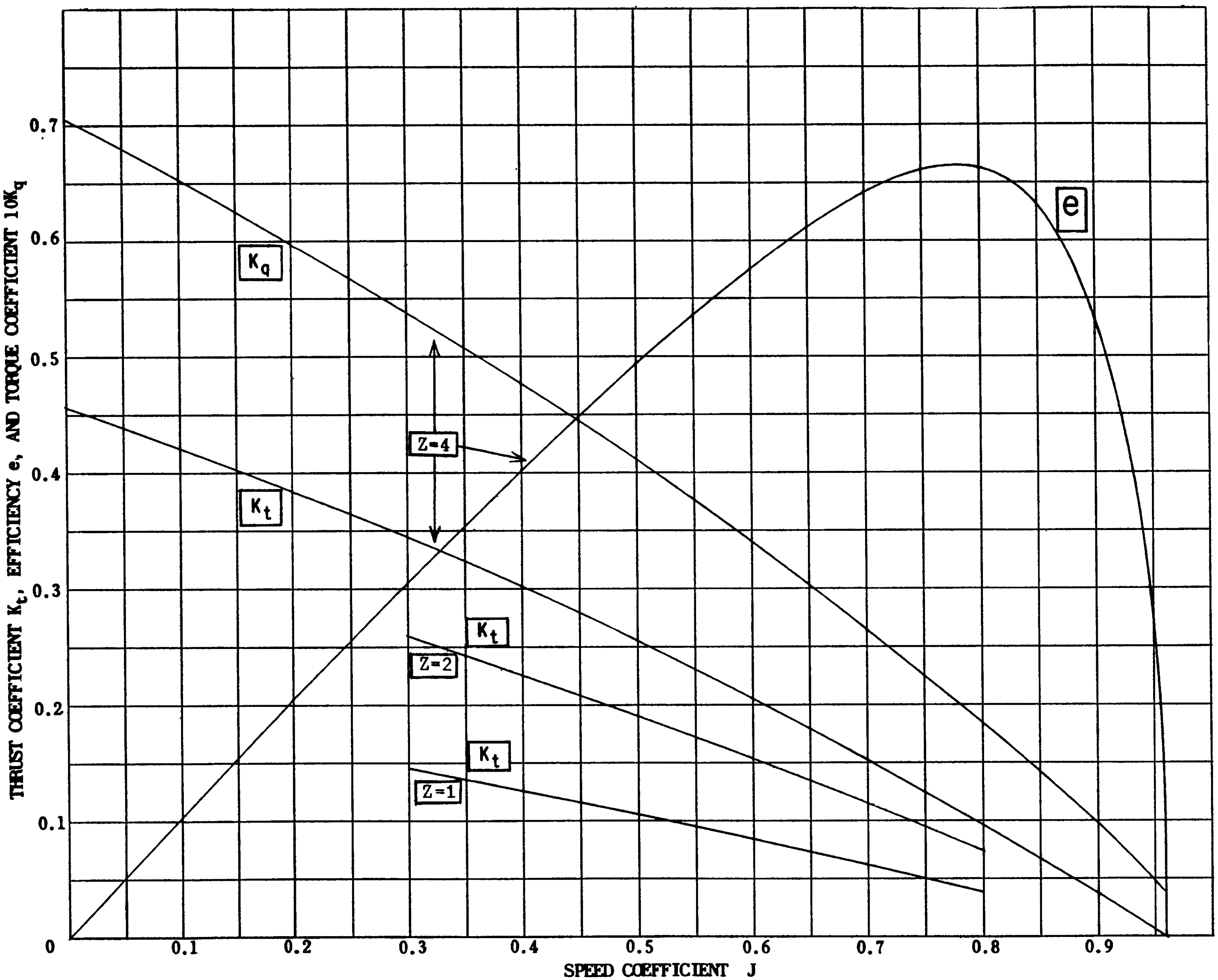

Figure 4 - Performance Characteristics of Propeller 3192

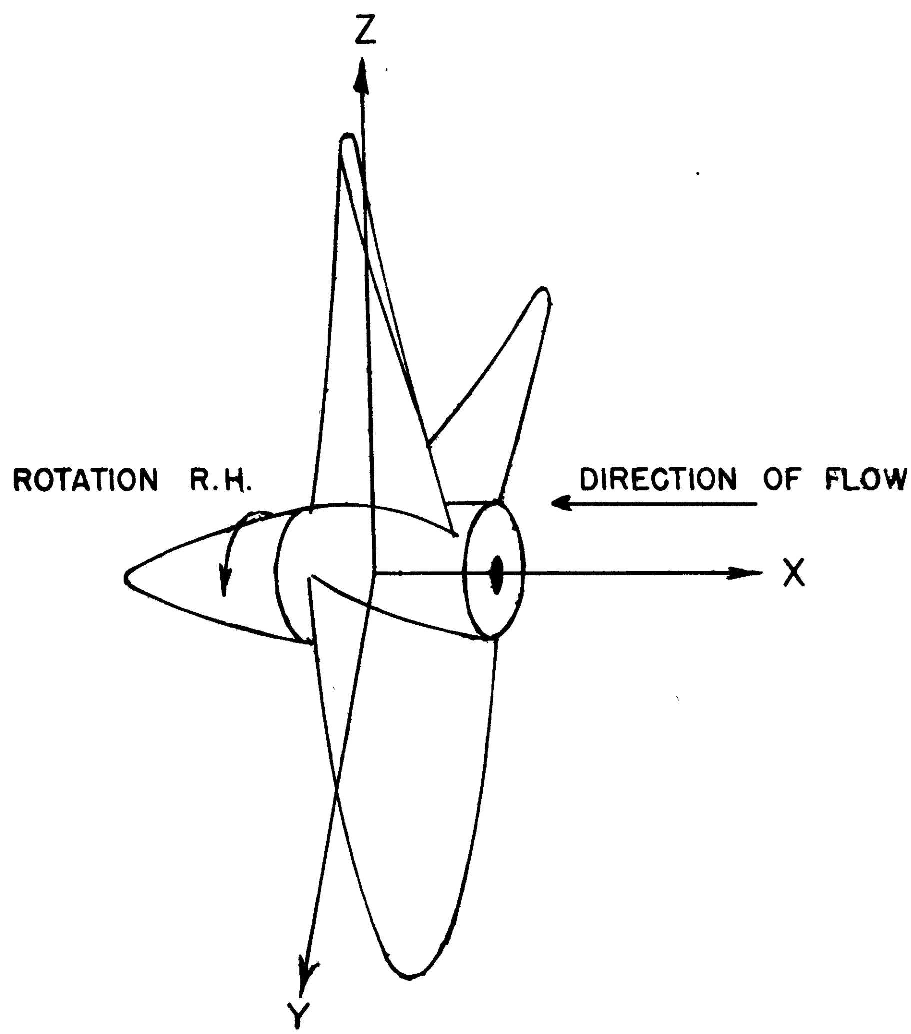

Figure 5 - Co-ordinate System

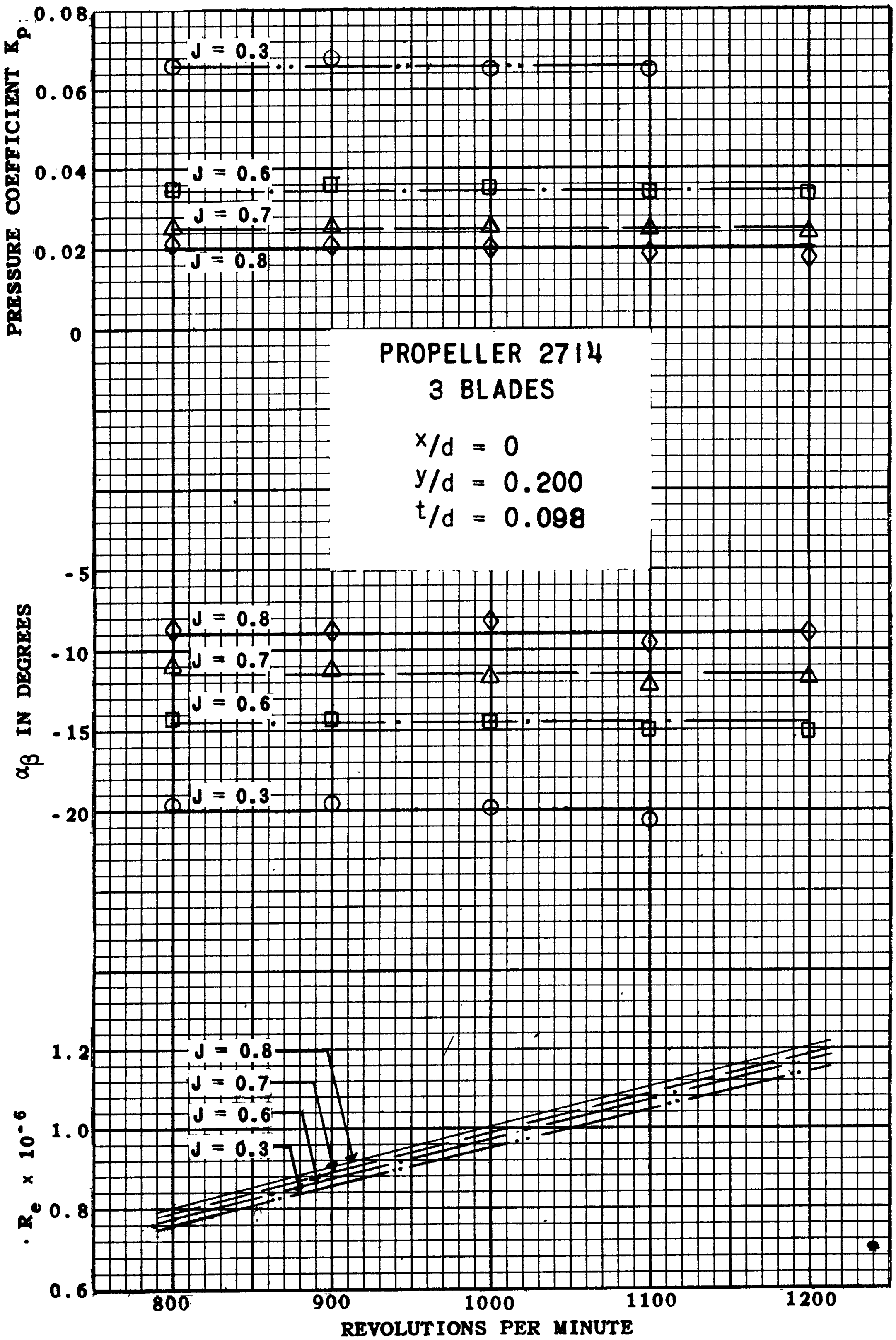

Figure 6 - Effect of RPM on Amplitude and Phase Angle of Oscillating Pressu

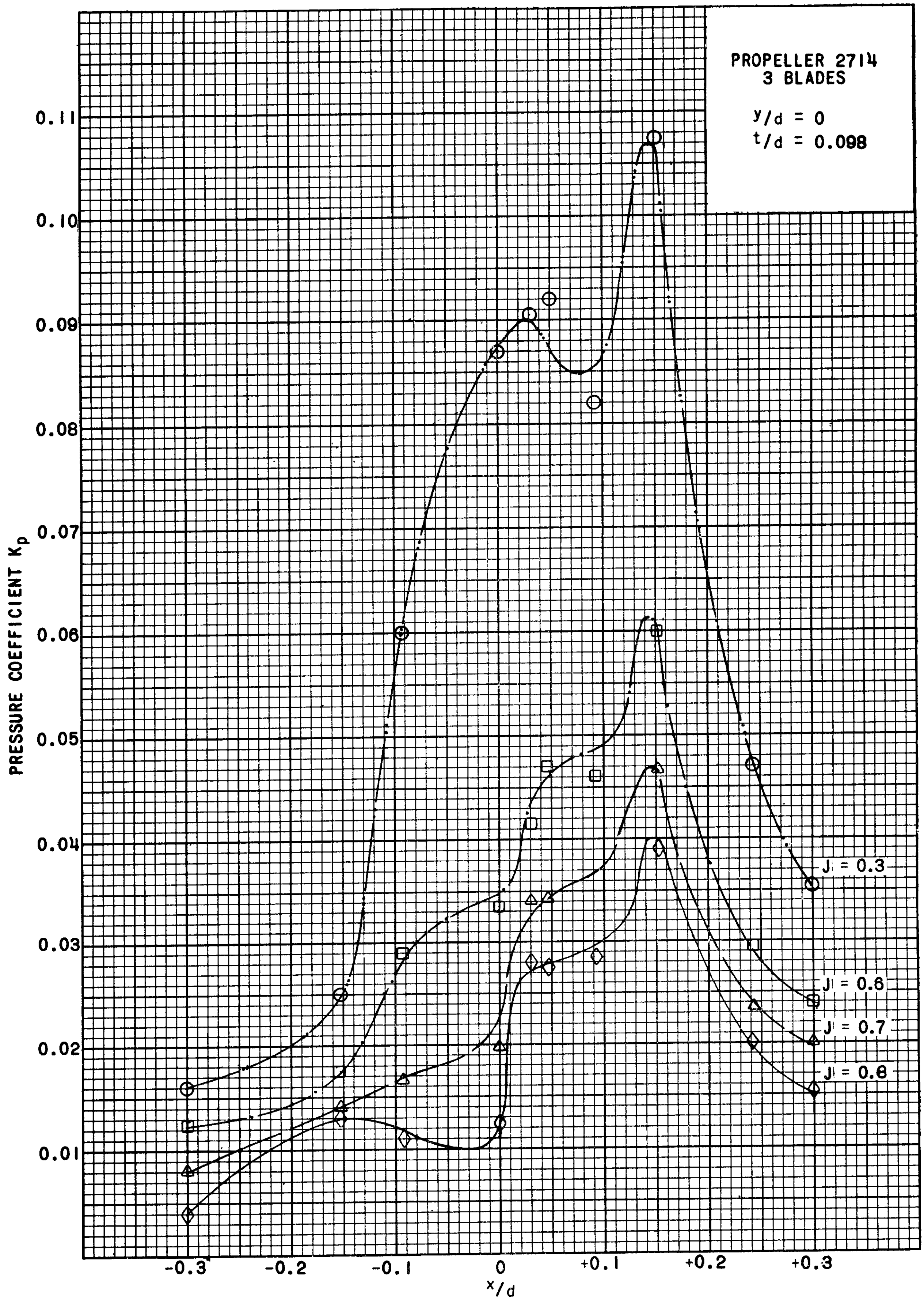

Figure 7 - Variation of Amplitude with Axial Distance

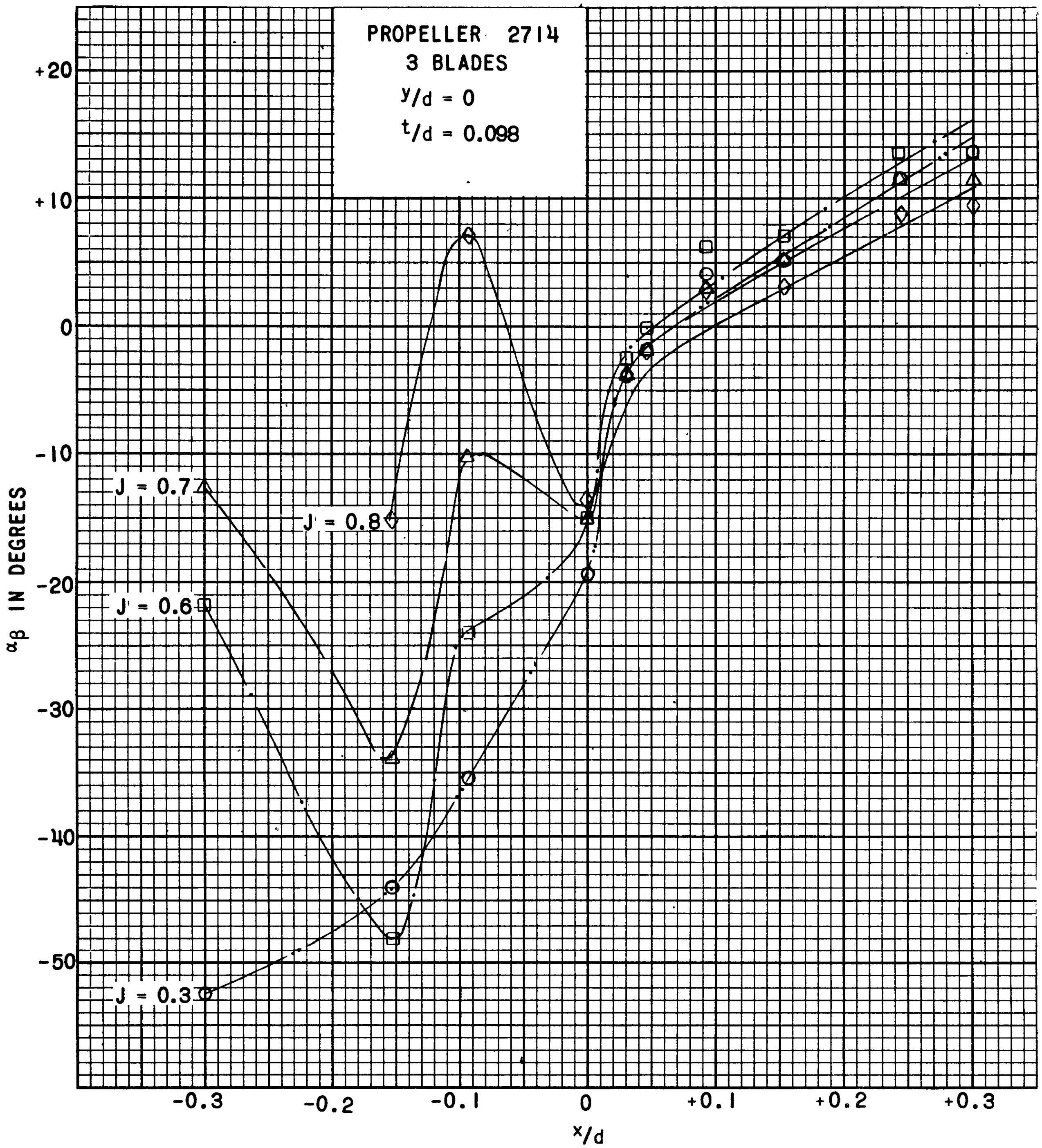

Figure 8 - Variation of Phase Angle with Axial Distance

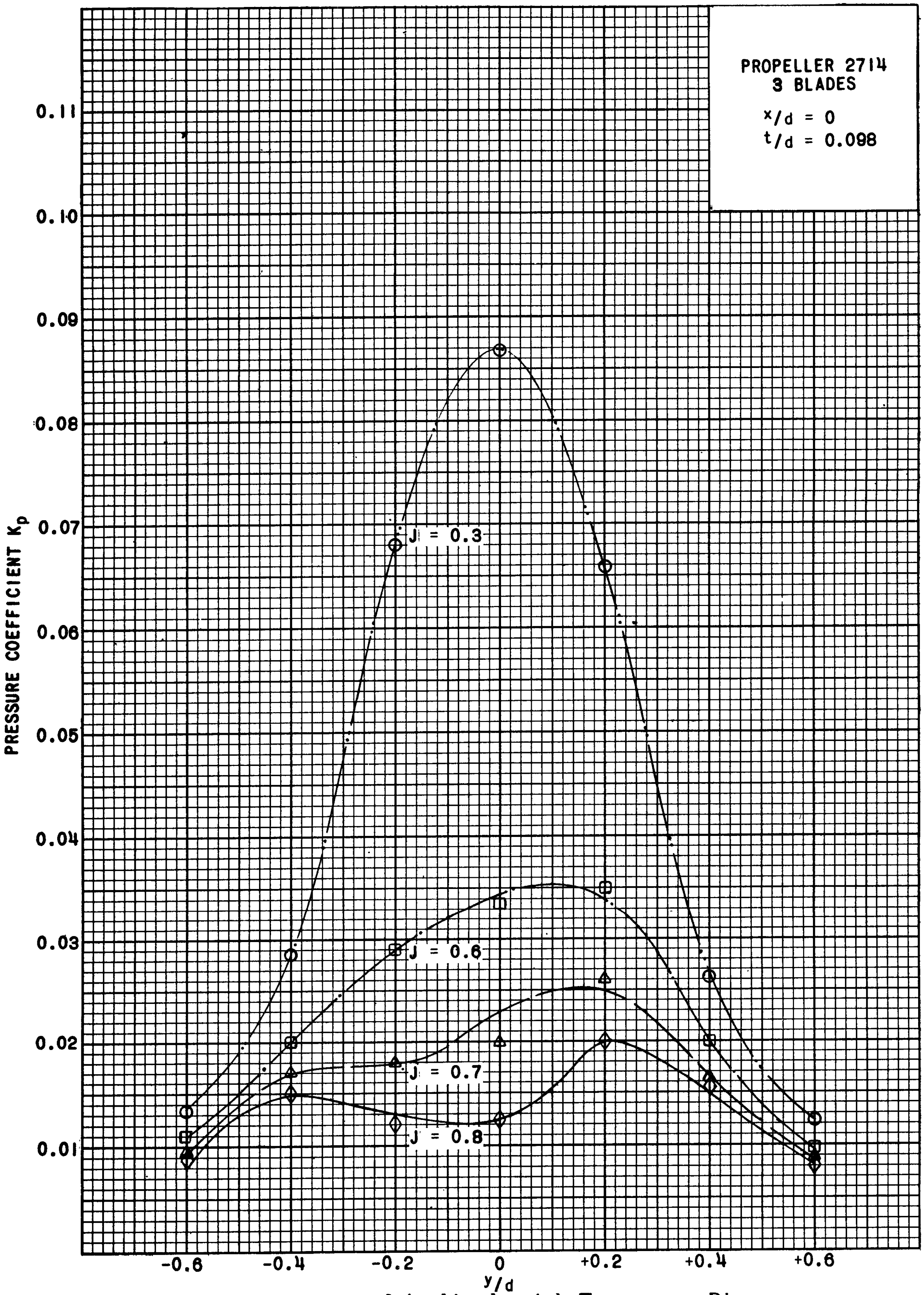

Figure 9 - Variation of Amplitude with Transverse Distance

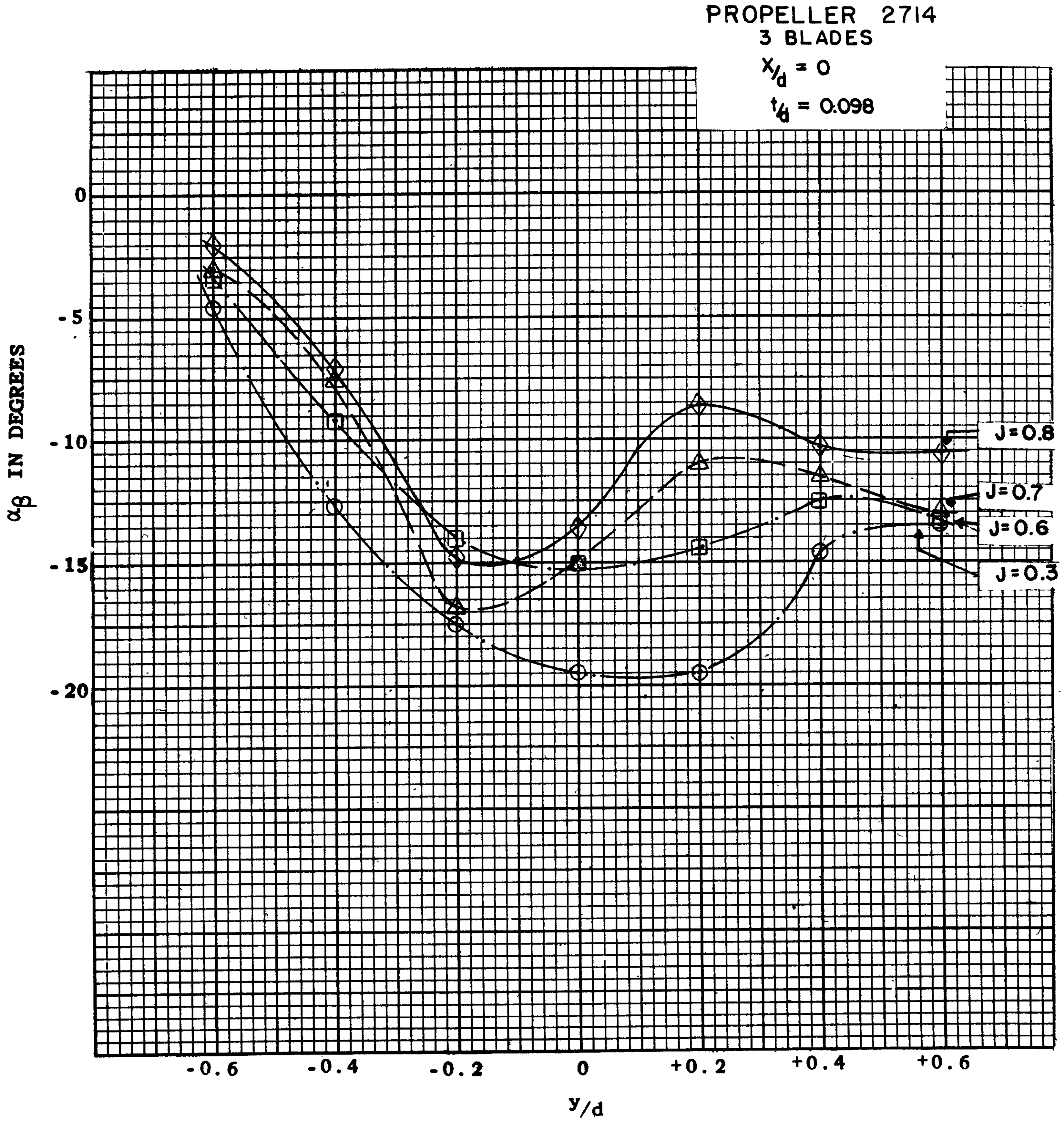

Figure 10 - Variation of Phase Angle With Transverse Distance

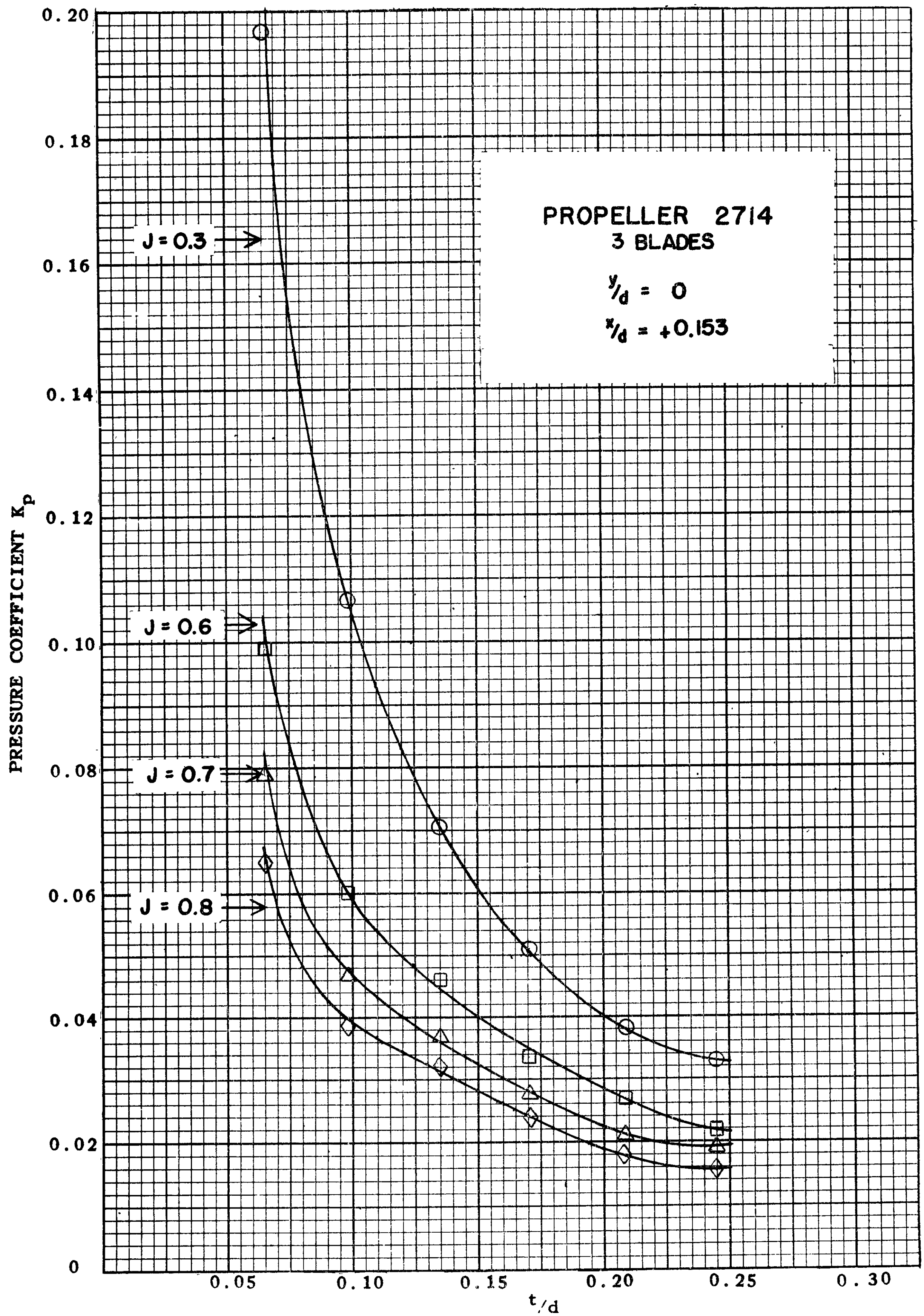

Figure 11 - Variation of Amplitude With Tip Clearance
(Ahead of the Propeller Plane)

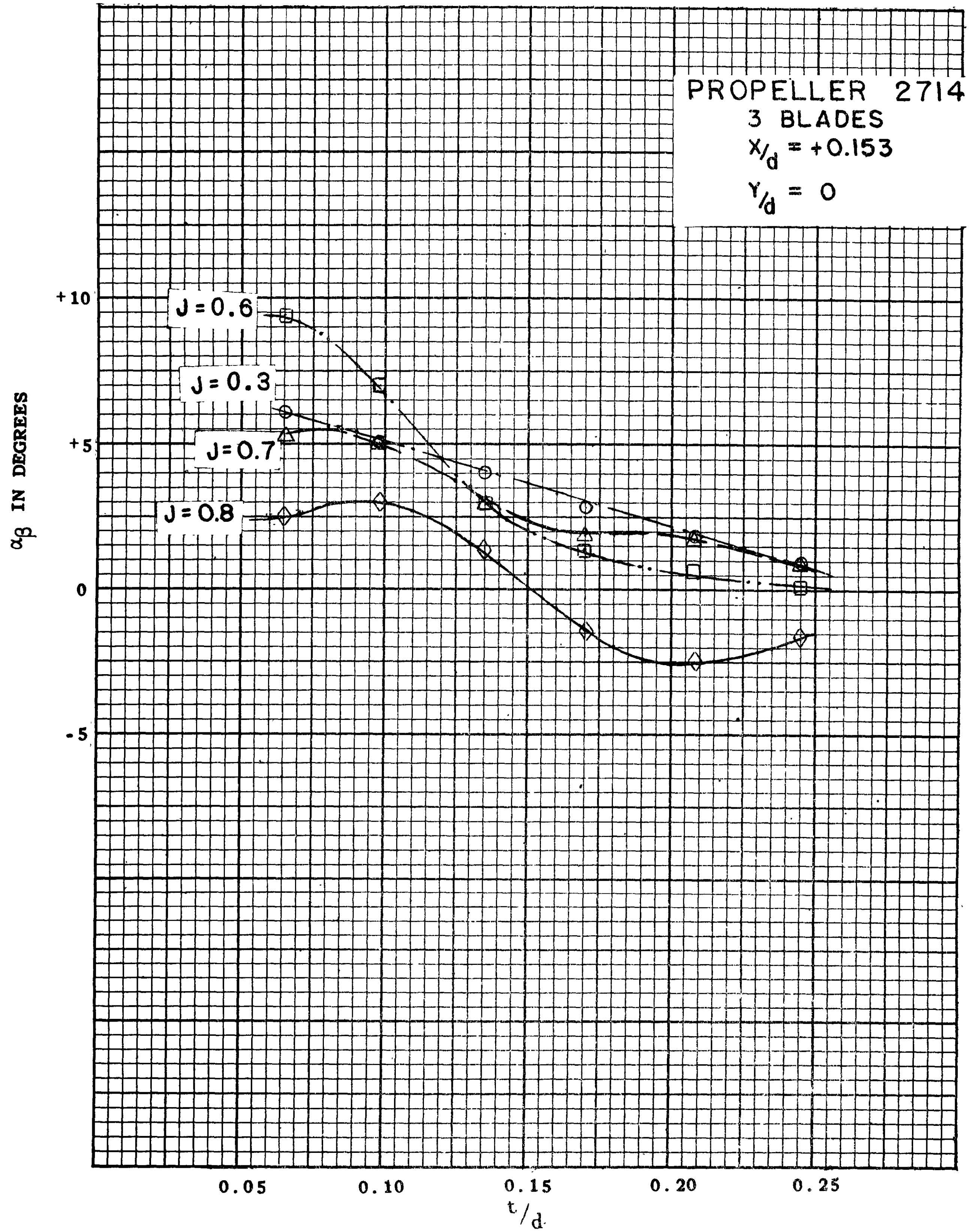

Figure 12 - Variation of Phase Angle With Tip Clearance
(Ahead of the Propeller Plane)

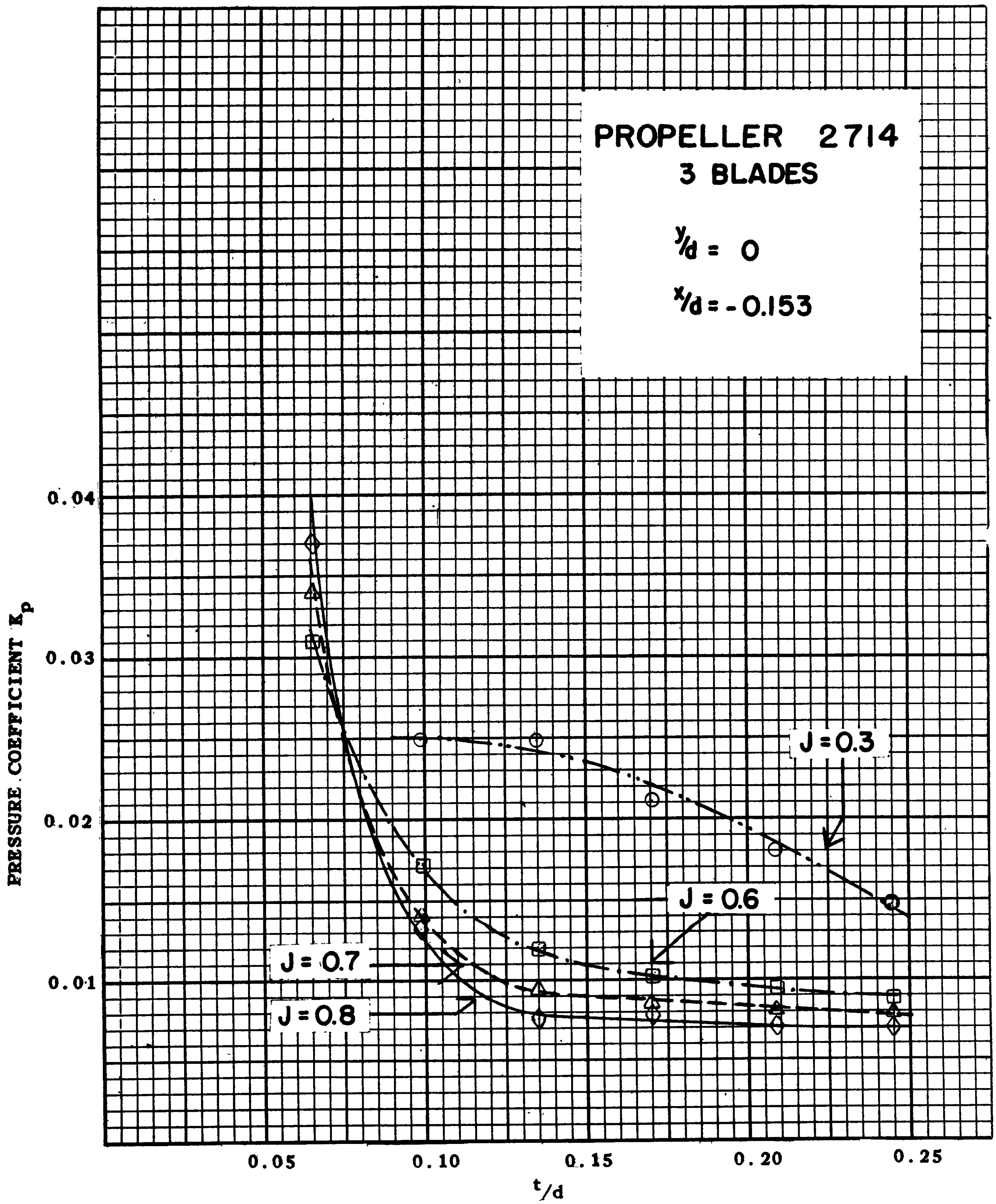

Figure 13 - Variation of Amplitude With Tip Clearance (Behind the Propeller Plane)

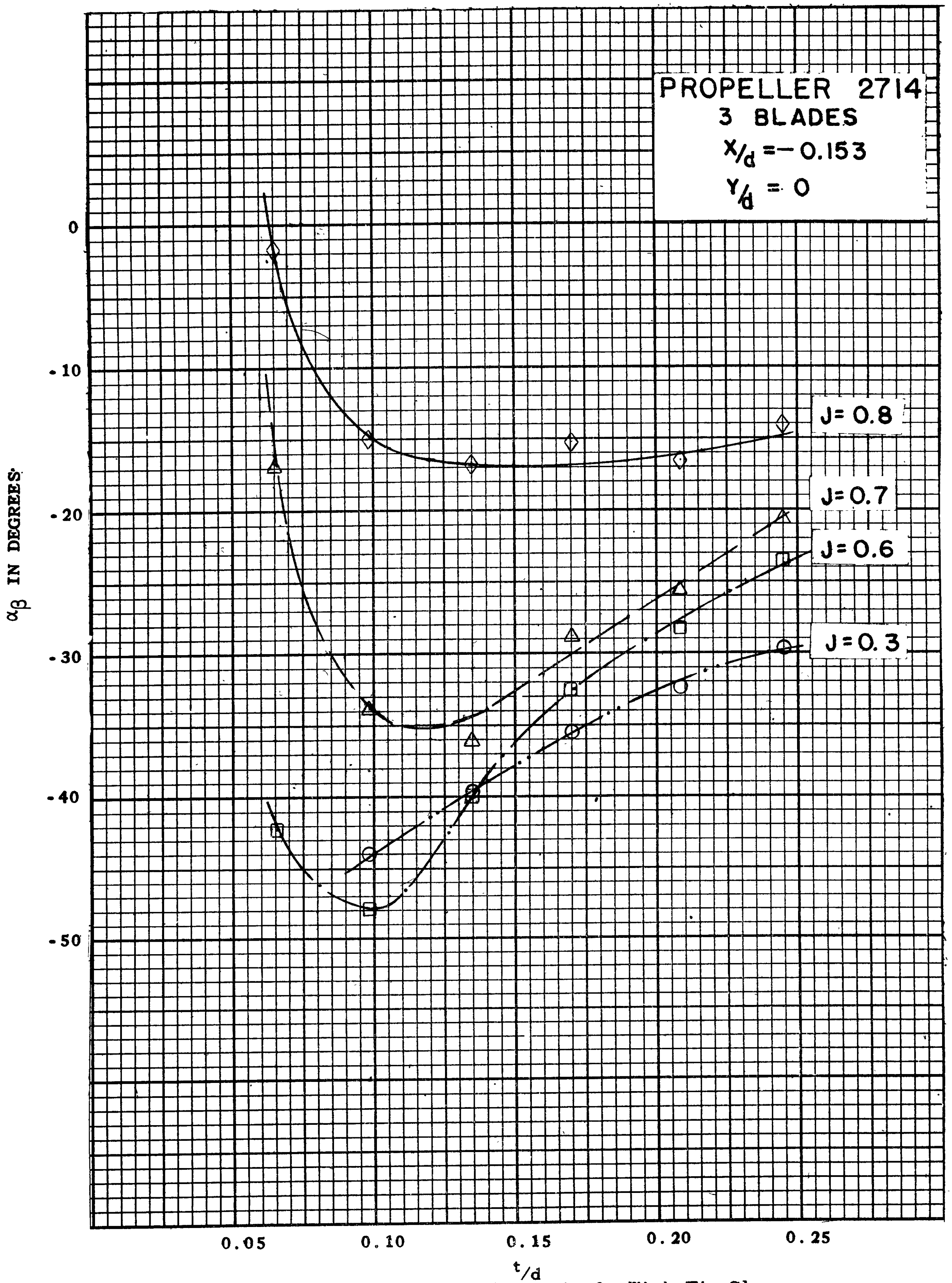

Figure 14 - Variation of Phase Angle With Tip Clearance
(Behind the Propeller Plane)

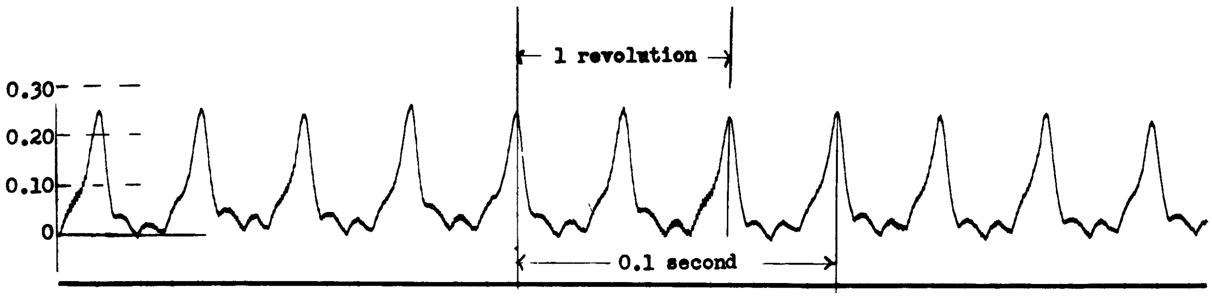

Figure 15-A 2-Bladed Propeller, J = 0.3

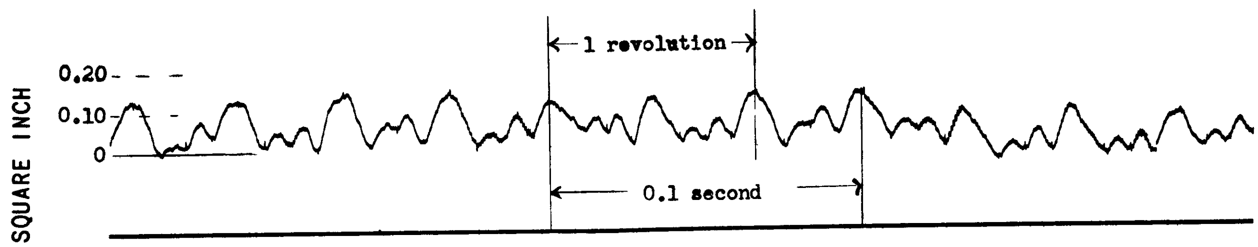

Figure 15-B - 2-Bladed Propeller, J = 0.7

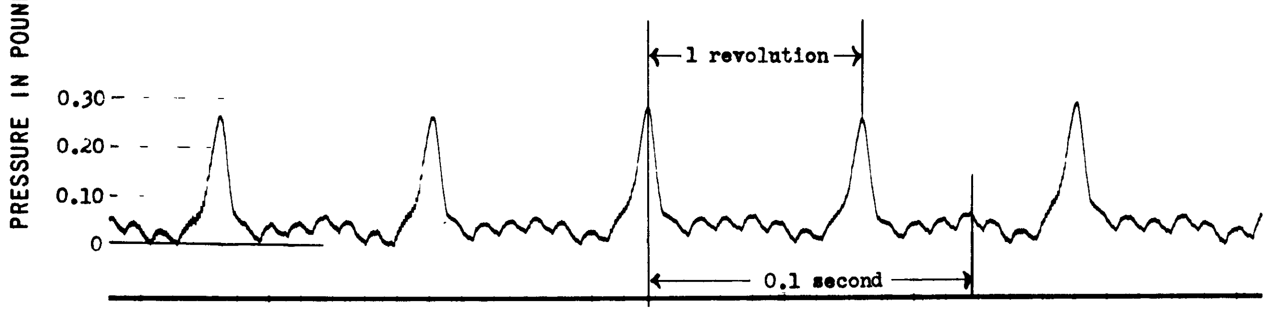

Figure 15-C - 1-Bladed Propeller, J = 0.3

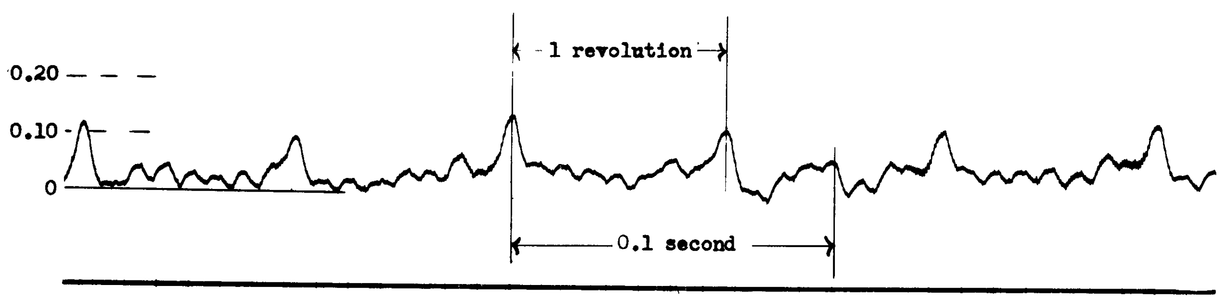

Figure 15-D - 1-Bladed Propeller, J = 0.7

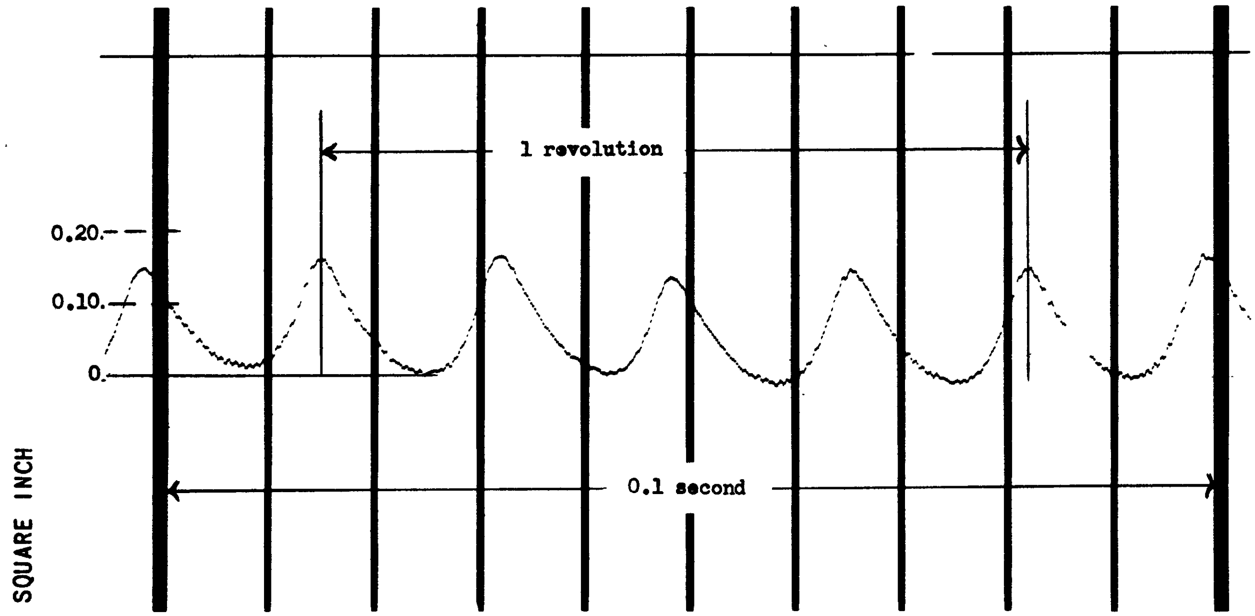

Figure 15-E - 4-Bladed Propeller, J = 0.3

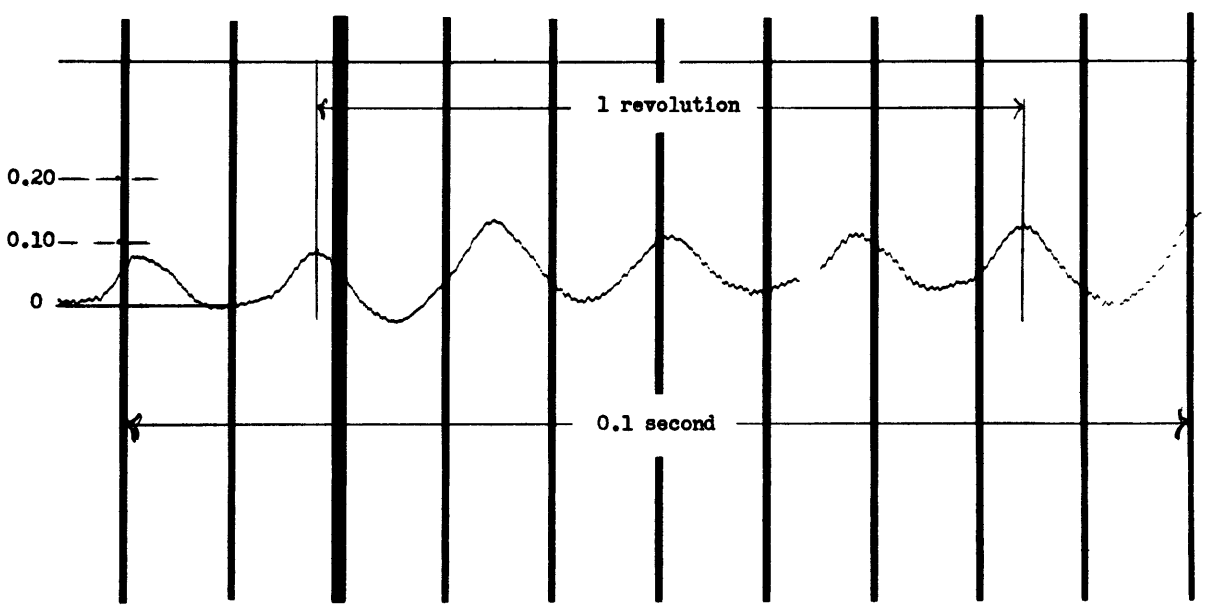

Figure 15-F - 4-Bladed Propeller, J = 0.7

Figure 15 - Typical Oscillograph Records

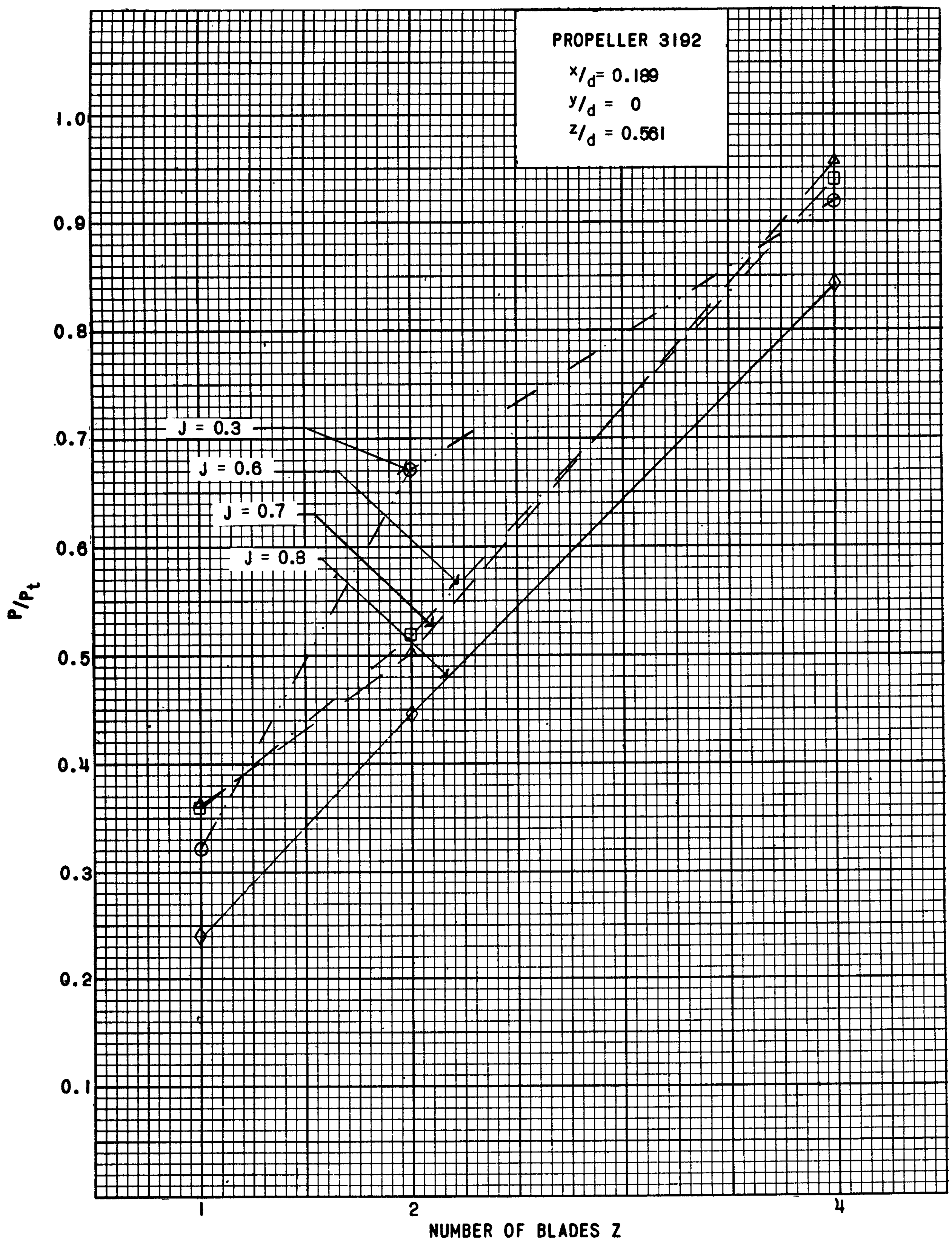

Figure 16 - Ratio of Blade Frequency Amplitude to Total Pressure Amplitude

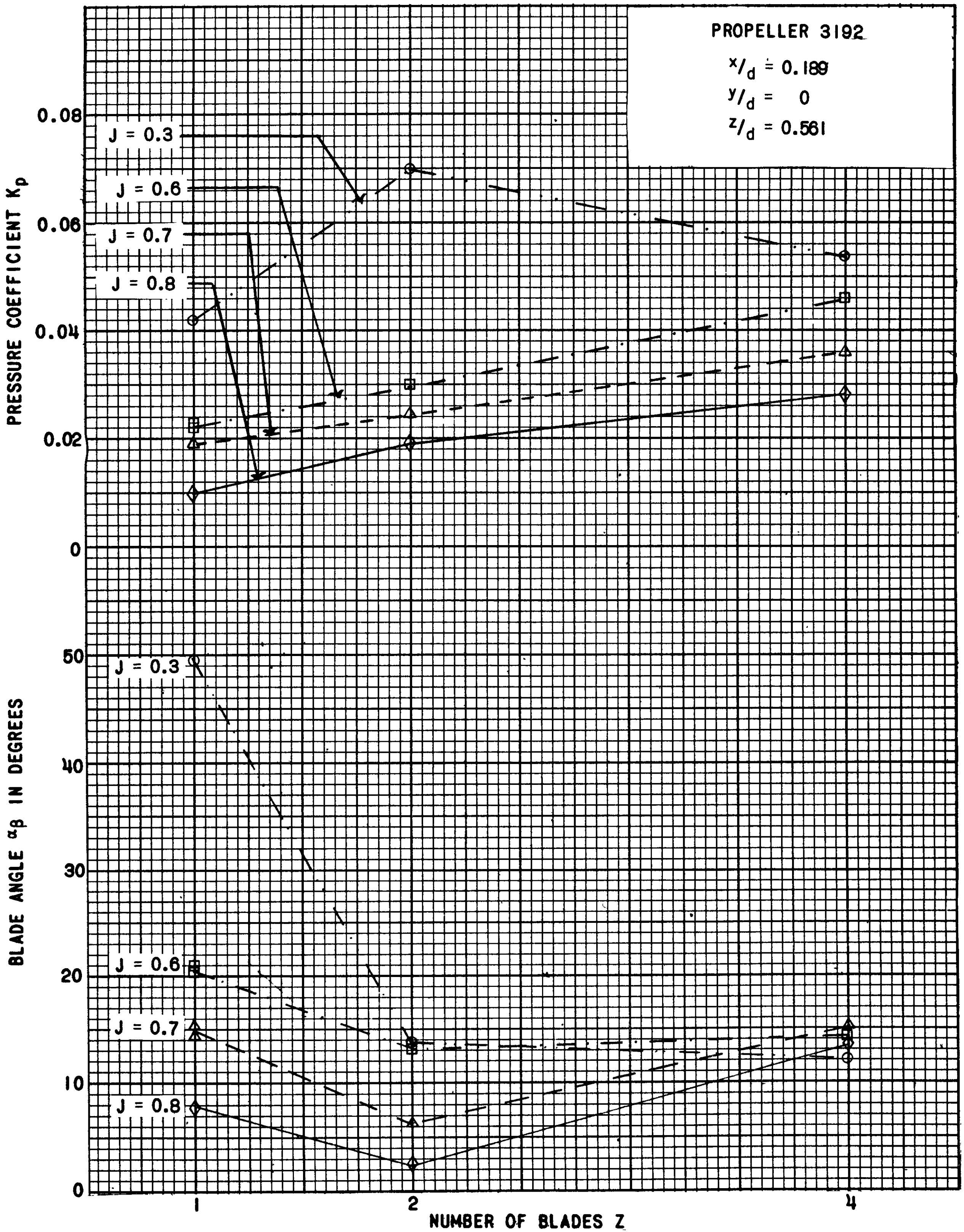

Figure 17 - Effect of Number of Blades on Amplitude and Phase of Oscillating Pressure

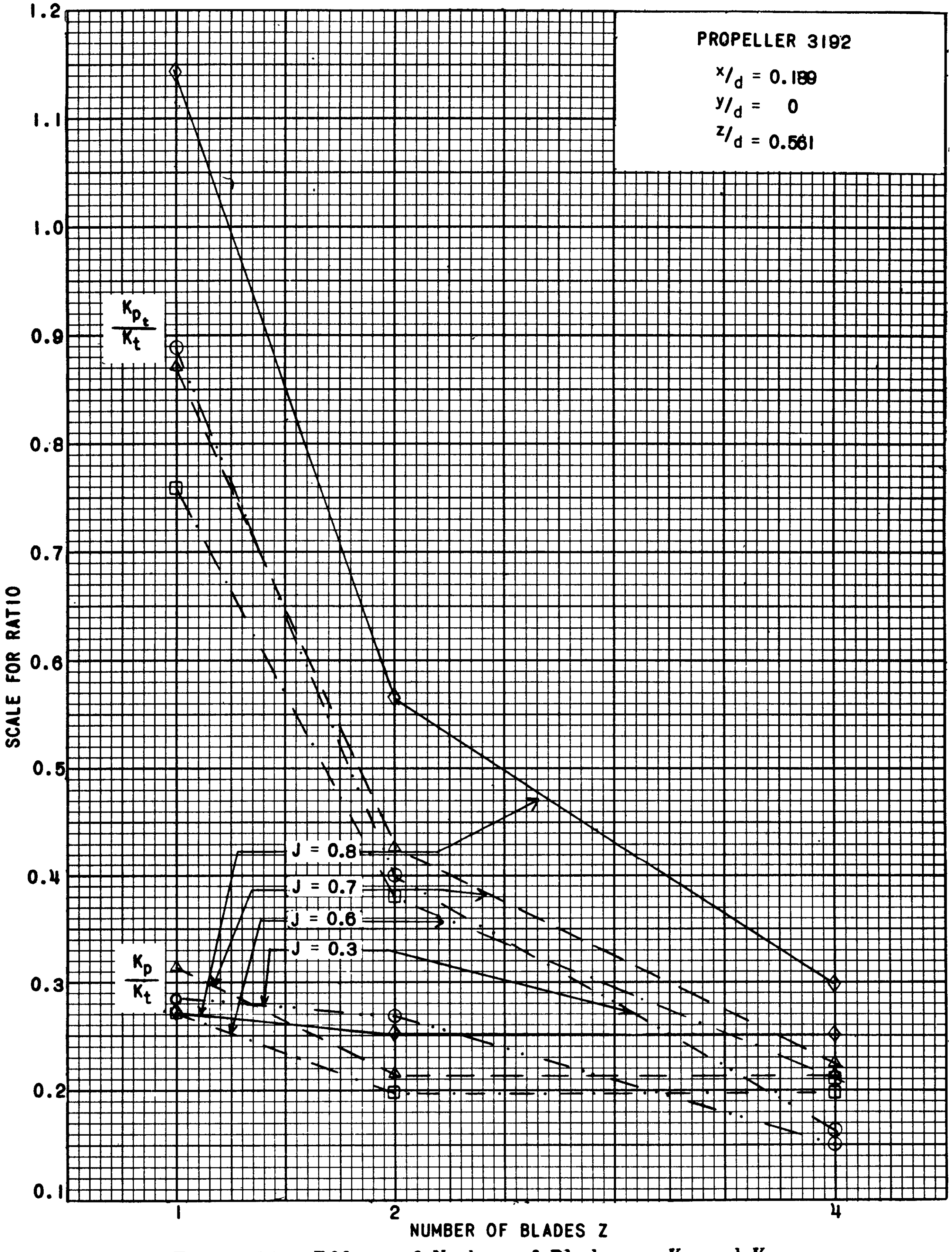

Figure 18 - Effect of Number of Blades on K_p and K_{p_t}
(Corrected for the Same Loading)

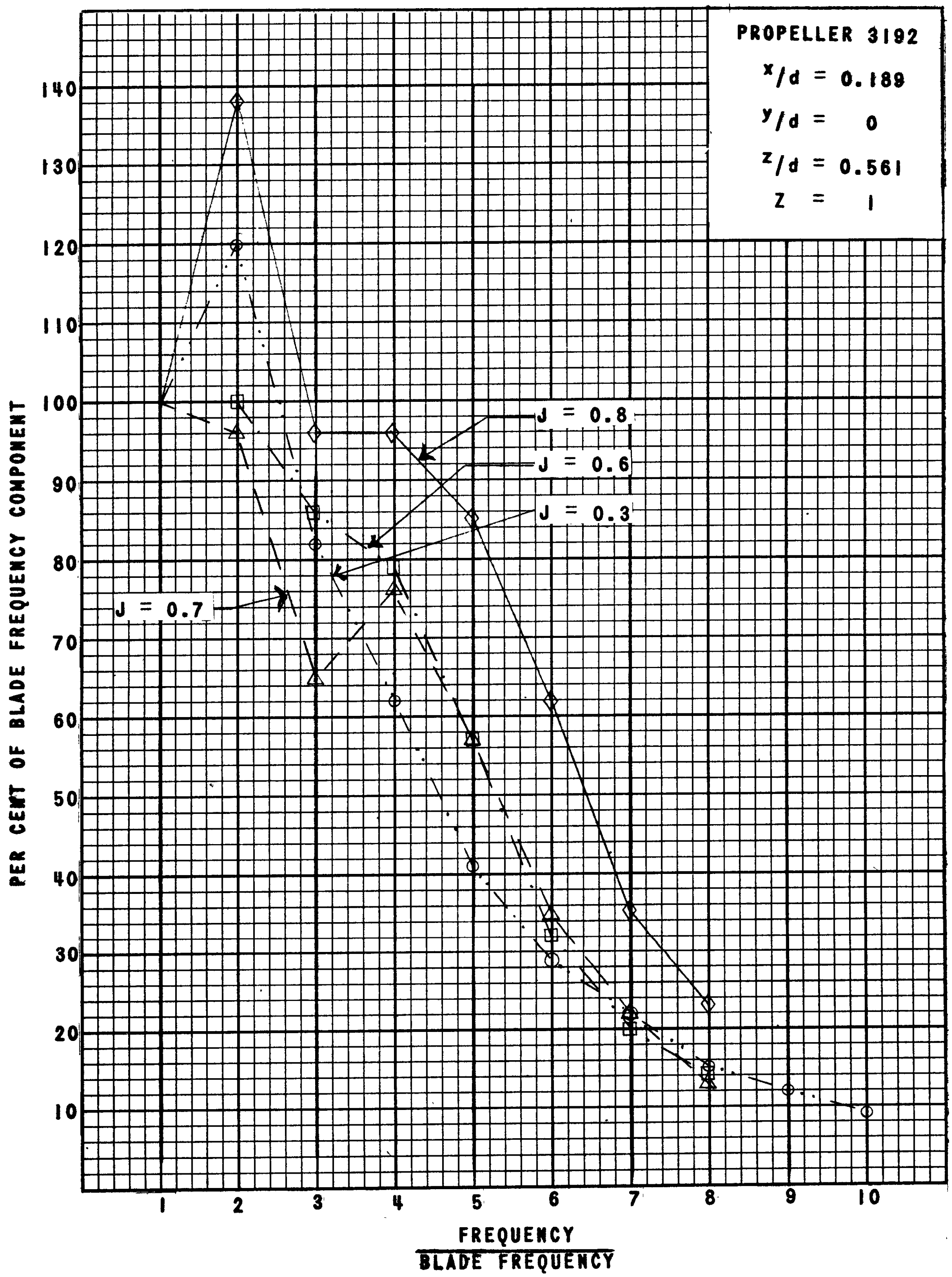

Figure 19 - Higher Harmonics for One-Bladed Propeller

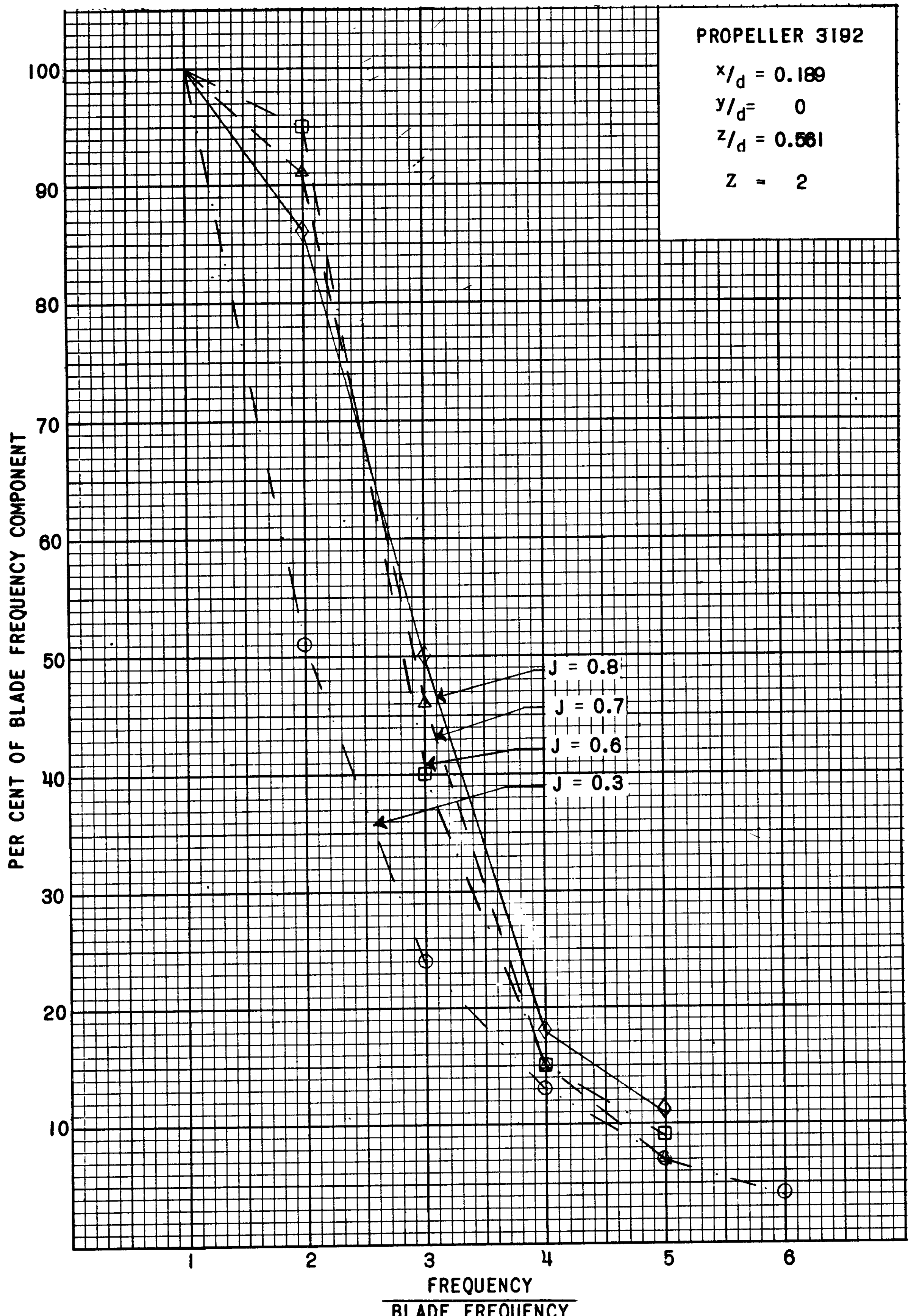

Figure 20 - Higher Harmonics for Two-Bladed Propeller

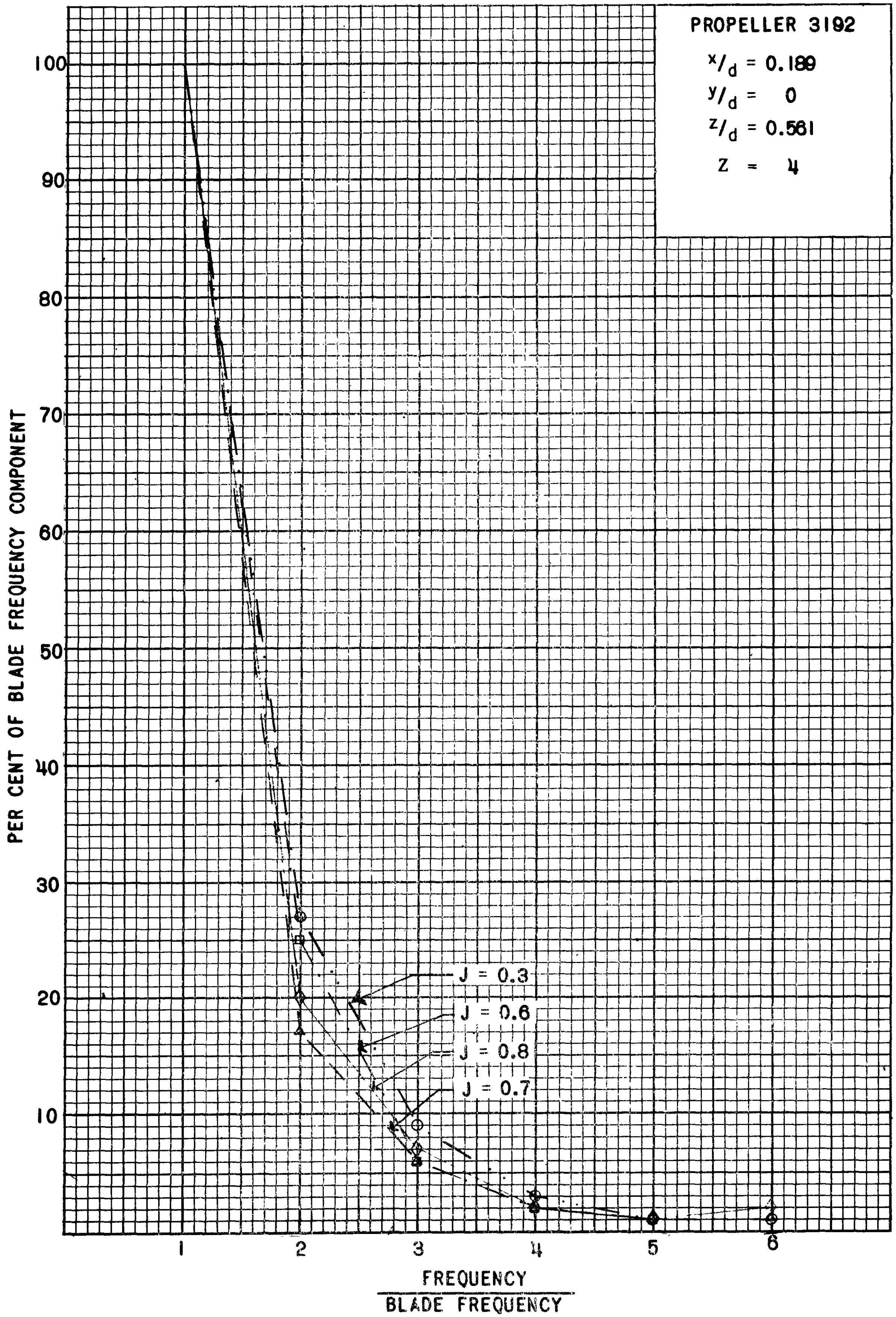

Figure 21 - Higher Harmonics for Four-Bladed Propeller

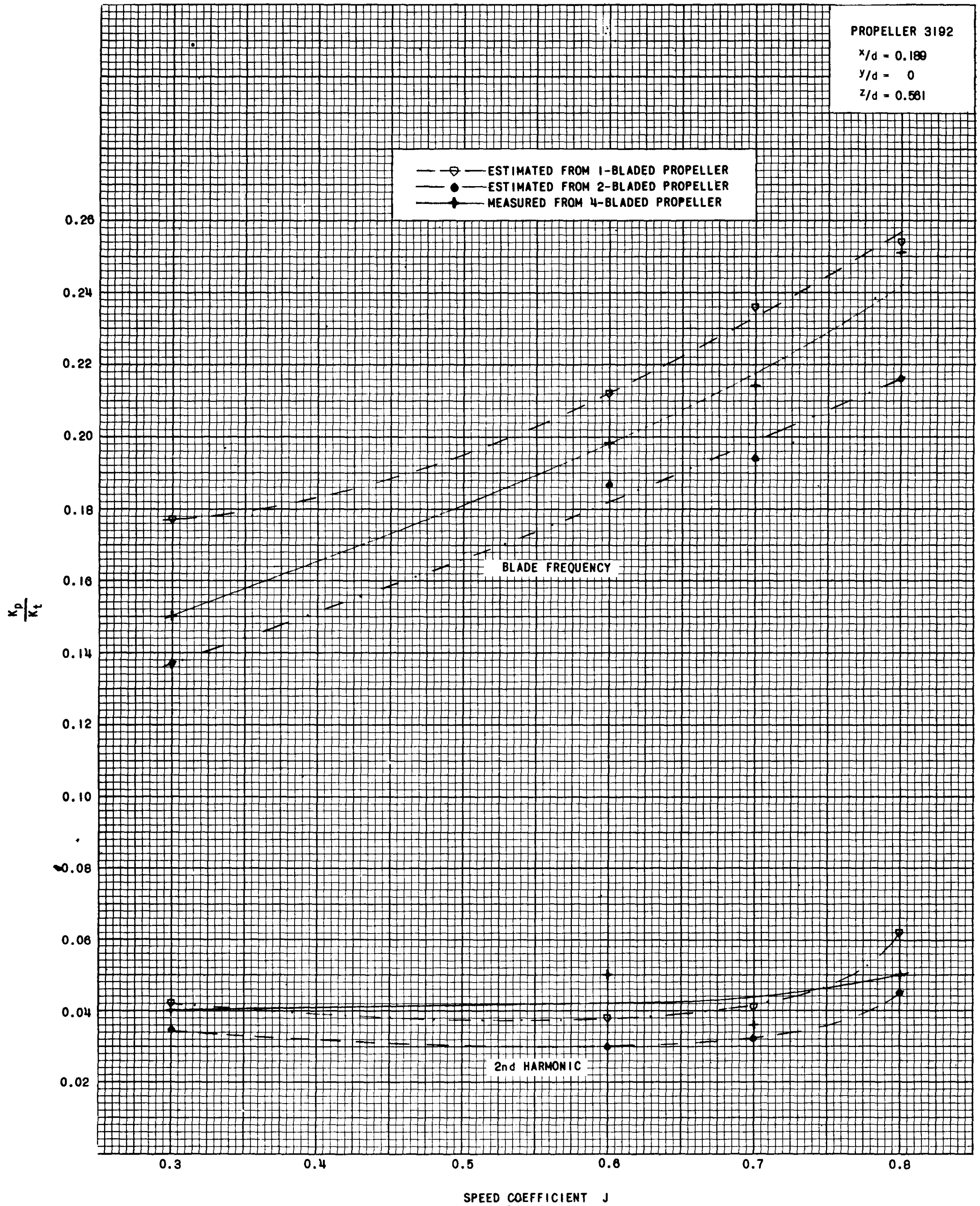

Figure 22 - Comparison Between Estimated and Measured Free-Space Oscillating Pressure for Four-Bladed Propeller

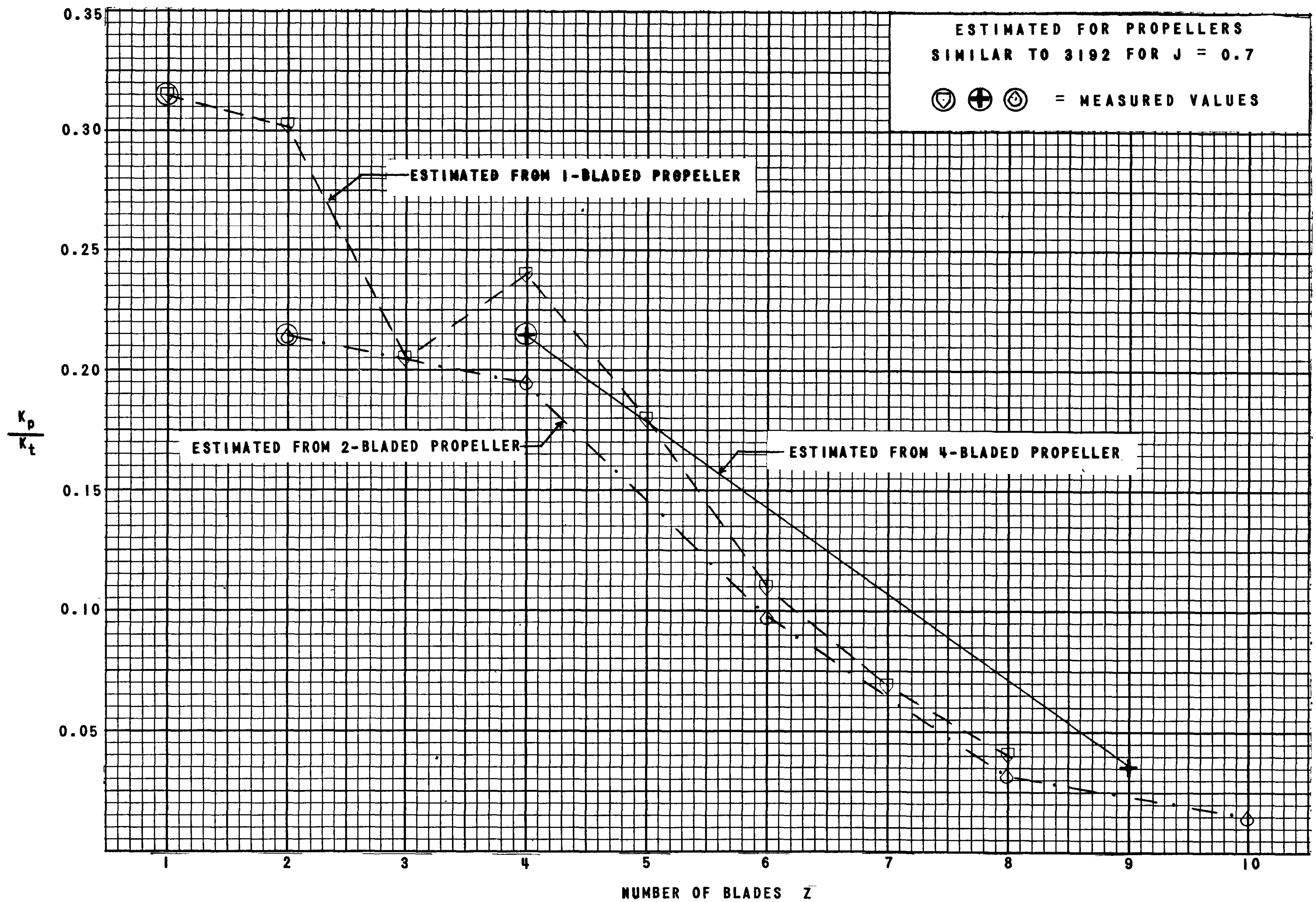

Figure 23 - Estimated Free-Space Oscillating Pressure for Propeller up to Z = 10

INITIAL DISTRIBUTION

Copies	
9	Chief, Bureau of Ships, Technical Library Code (312), for distribution 5 Technical Library 1 Civilian Consultant to the Chief (Code 106) 1 Preliminary Design (Code 421) 1 Hull Design (Code 440) 1 Propellers and Shafting (Code 554)
1	Chief of Naval Research, Fluid Mechanics Branch, Code 438
1	Ordnance Research Laboratory, Pennsylvania State University University Park, Pennsylvania
1	Superintendent, Admiralty Experiment Works, Haslar, Gosport, Hants, England
1	Superintendent, Ship Division, National Physical Laboratory, Teddington, Middlesex, England
1	Director, Netherlands Scheepsbouwkundig Proefstation Wageningen, Holland
1	Director, Statens Skeppsmodeltanken, Tyholt, Trondheim, Norway
1	Director, Canal de Experiencias Hidrodinamicas, El Pardo, Madrid, Spain
1	Experimental Towing Tank, Stevens Institute of Technology, Attn: Dr. J. Breslin, 711 Hudson Street, Hoboken, New Jersey
1	Head, Department of Naval Architecture and Marine Engineering, Massachusetts Institute of Technology Cambridge 39, Massachusetts
1	British Shipbuilding Research Association, Chesterfield Gardens, Curzon St., London W1, England
1	Director, Hamburg Model Basin, Hamburg 33, Germany
1	Karlstads Mekaniska Werkstad, Kristinehamn, Sweden
1	Eastern Research Group, 215 Montague St., Brooklyn 1, New York, Attn: Dr. L. Meyerhoff
1	Director, Hydrodynamics Laboratory, California Institute of Technology, Pasadena 4, California
1	Chief, Division of Ship Design, Office of Ship Construction, U. S. Maritime Administration, Washington 25, D. C.
3	Canadian Joint Staff, 2450 Massachusetts Ave., N. W., Washington 6, D. C.
9	British Joint Services Mission (Navy Staff), P. O. Box 165, Benjamin Franklin Station, Washington, D.C.